

3. SITE 322

The Shipboard Scientific Party¹

SITE DATA

Position: 60°01.45'S, 79°25.49'W (Eastern end of Bellingshausen Abyssal Plain)

Water Depth: 5026 corrected meters, echo sounding. 5026 drill pipe measurement.

Number of Holes: 1

Number of Cores: 14

Penetration: 544 meters

Total Length of Cored Section: 125.5 meters

Total Core Recovered: 34.22 meters

Percentage Core Recovered: 27.4%

Oldest Sediment Cored:

Depth Subbottom: 513.3 meters

Nature: Brown clay

Age: ?Oligocene to early Miocene

Velocity: 2 km/sec

Basement:

Depth subbottom: 513.3 meters

Penetration: 30.7 meters

Nature: Basalt.

Velocity: 5 km/sec

Principal Results: Thirty-one meters of terrigenous clay, silt, and sand, and 3 meters of basalt were recovered from 544 meters drilled into the eastern end of the Bellingshausen Abyssal Plain. The detrital and terrigenous sediments range in age from Pliocene to early Miocene; the oldest sediment is 1 meter of pelagic brown clay recovered from just above basalt; it is early Miocene to ?Oligocene in age. All of the sediment appears to have been deposited beneath the depth of carbonate compensation. Little ice-rafted detritus was recognized at this site. The basalt (3 m

recovered from 30 m penetration) is similar to mid-ocean ridge extrusives with glassy veins and hyaloclastite breccia. Seismic profiles at this site show gently undulating, and locally discontinuous lenticular reflectors that become less intense with increasing depth. Acoustic basement cannot be recognized except as a region devoid of reflecting horizons. Generally, good size sorting of clastic material and the lenticular, discontinuous, attitudes of most reflecting horizons suggest that the sediment was originally deposited as distal turbidites and reworked by bottom currents.

BACKGROUND AND OBJECTIVES

Background

Site 322 lies near the eastern end of the Bellingshausen Abyssal Plain (Figures 1 and 2). A few tens of kilometers to the north is rough topography associated with the Hero Fracture Zone area and the flanks of the Chile Ridge; to the west lie the Tula and Eltanin Fracture zones and the Pacific-Antarctic Ridge (Tucholke and Houtz and Herron and Tucholke, both this volume). Water depths throughout the region exceed 4000 meters and in the vicinity of the site exceed 5000 meters. Water depths less than 4000 meters occur to the northeast near South America, to the east in the Drake Passage, and to the southeast near the Antarctic Peninsula. Tectonically, the site lies in the deep oceanic part of the Antarctic plate. A seismic profile through the site (*Eltanin-43*, 1900 hr, 26 April 1970, Figures 3 and 4) indicates a smooth abyssal plain underlain by a few hundred meters of sediment resting upon a rough basement.

The regional geology of the Southeast Pacific Basin and the adjacent land masses is poorly known. The Andes Mountains of South America and the coastal zone of West Antarctica mark segments of the Pacific continental margin of Gondwanaland (Craddock, 1975), and recurrent orogenic cycles from the early Paleozoic through the latest Mesozoic have been recognized. The modern Andean chain, at 9000 km the longest on earth, serves as an ideal model for the cordilleran-type range (Gansser, 1973b); it is commonly explained as the result of oceanic plate subduction beneath an active continental margin, but Gansser (1973a) argues that block-faulting rather than compression has predominated in the Andes during the Cenozoic. The intersection of the Chile Ridge separates the active central Andes from the relatively quiescent southern Andes. The central Andes are marked by many active volcanoes and earthquakes, but the southern Andes contain only two active volcanoes, and earthquakes are few and widely spaced (Gonzalez-Ferran, 1972). The Scotia Arc probably formed by Cenozoic disruption of an earlier, nearly linear belt

¹Charles D. Hollister, Woods Hole Oceanographic Institution, Woods Hole, Massachusetts (Co-chief scientist); Campbell Craddock, University of Wisconsin, Madison, Wisconsin (Co-chief scientist); Yuri A. Bogdanov, P.P. Shirshov Institute of Oceanology, U.S.S.R. Academy of Sciences, Moscow, U.S.S.R.; N. Terence Edgar, Scripps Institution of Oceanography, La Jolla, California (Present address: U.S. Geological Survey, Reston, Virginia); Joris M. Gieskes, Scripps Institution of Oceanography, La Jolla, California; Bilal U. Haq, Woods Hole Oceanographic Institution, Woods Hole, Massachusetts; James R. Lawrence, Lamont-Doherty Geological Observatory, Columbia University, Palisades, New York; Fred Rögl, Eidg. Technische Hochschule, Zurich, Switzerland (Present address: Naturhistorisches Museum, Vienna, Austria); Hans-Joachim Schrader, Institut und Museum der Universität Kiel, Kiel, Germany; Brian E. Tucholke, Lamont-Doherty Geological Observatory, Columbia University, Palisades, New York; Walter R. Vennum, Sonoma State College, Rohnert Park, California; Fred M. Weaver, Florida State University, Tallahassee, Florida; Vasily N. Zhivago, P.P. Shirshov Institute of Oceanology, U.S.S.R. Academy of Sciences, Moscow, U.S.S.R.

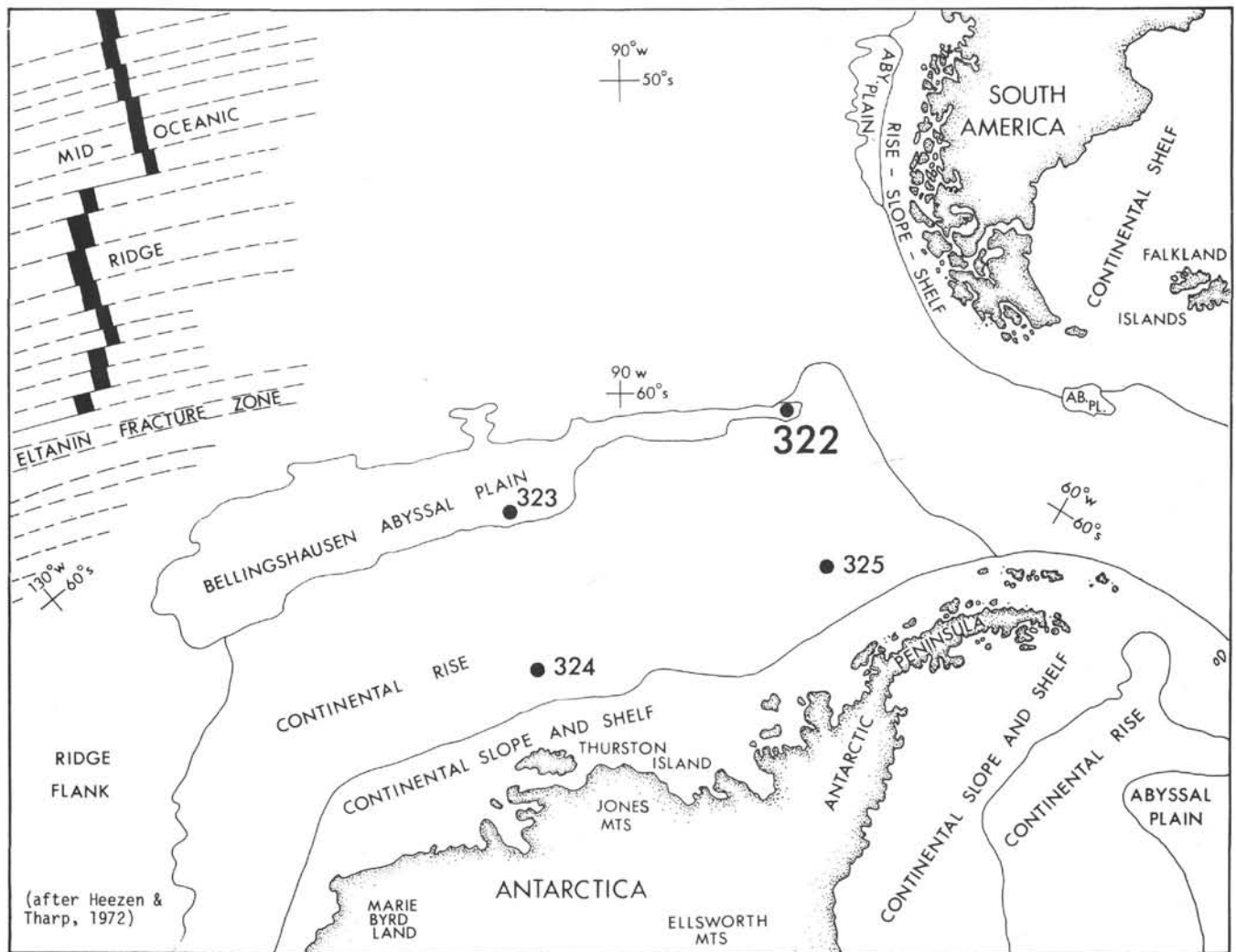


Figure 1. Location of Site 322.

which connected South America and the Antarctic Peninsula during the Mesozoic (Dalziel and Elliot, 1973). Paleozoic and Mesozoic orogenic cycles have formed widespread igneous plutons and deformed metasedimentary and metavolcanic rocks in the Antarctic Peninsula and westward along the Antarctic coast (Adie, 1970; Craddock, 1972). Although there has been extensive Cenozoic volcanic activity in this part of Antarctica, there is very little evidence for Cenozoic compression and folding. Except for a few earthquakes in the western Drake Passage, the Antarctic plate appears to be aseismic at present.

The tectonic relationships and interactions between the Antarctic plate and the Scotia Arc, the southern Andes, and the Chile Ridge are little understood. In particular, no firm evidence is available from which to establish the age of the sea floor under the Southeast Pacific Basin. For the vicinity of Site 322 three models can be considered, based on the limited magnetic data available. Pitman et al. (1968) show the known magnetic anomalies which parallel the East Pacific Ridge; projection of their data suggests a Mesozoic basement, probably early Cretaceous in age. Herron

(1971) interprets the Chile Ridge as a spreading axis, and if the crust at Site 322 formed by southwestward spreading away from this axis, an early Tertiary age is probable. Griffiths and Barker (1972) describe a northeast-trending spreading axis in the Drake Passage; if the Site 322 crust came from this source, a late Cenozoic age is possible.

During the last decade geologists have developed a strong interest in ophiolites. With the emergence of the concepts of sea-floor spreading, subduction, and obduction, it became evident that ophiolites might represent slices of ancient oceanic crust pushed onto continents along active continental margins. Obviously, the evaluation of this hypothesis requires information about modern oceanic crust.

Little is known of the sediments beneath the Southeast Pacific Basin and the history of physical and biological events which they may record (Goodell et al., 1973). Two cores containing graded coarse sand layers (L-DGO RC15-67 and V18-17) taken within 100 km of Site 322 suggest that the abyssal plain is underlain by flat-lying turbidite sediments. Site 322 lies near the western entrance to the Scotia Sea and close to the axis

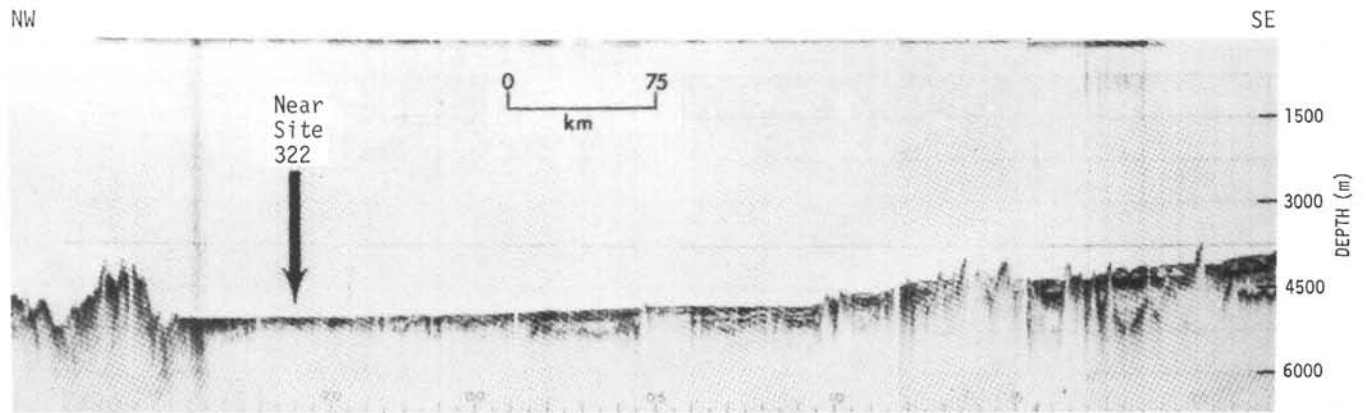


Figure 3. A northwest-southeast seismic profile (Eltanin-43) across the eastern end of the Bellingshausen Abyssal Plain near the Hero Fracture Zone. The Antarctic continental rise is on the right. The arrow is two miles west of Site 322.

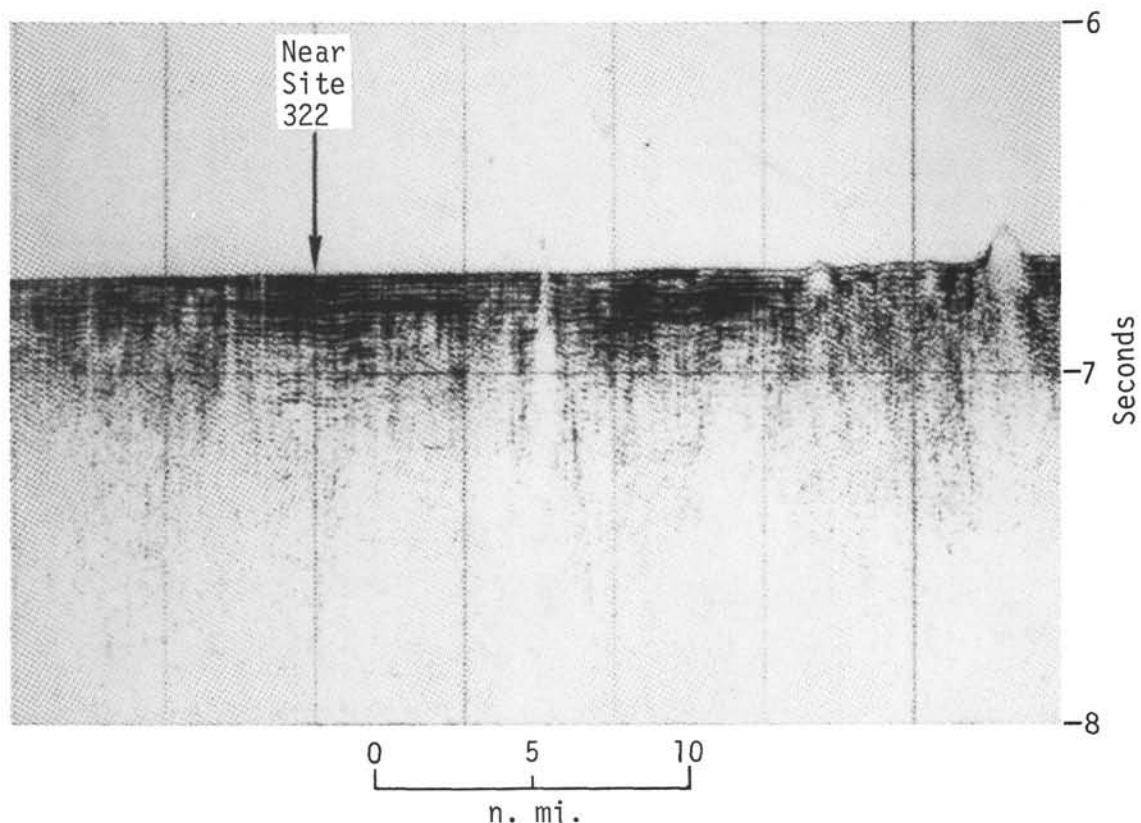


Figure 4. Enlargement of Eltanin-43 seismic profile near Site 322. See Figure 6 for location.

of the Antarctic Circumpolar Current which flows eastward at a rate of more than 2000 million m^3/sec (Gordon, 1967, 1972; Reid and Nowlin, 1971). Weissel and Hayes (1972) infer from magnetic anomalies that oceanic crust began forming between East Antarctica and Australia about 55 m.y.B.P.; this may be the earliest date at which the present circumpolar circulation pattern could have formed. Kennett et al. (1972) report a regional unconformity of Oligocene age in the southwestern Pacific Ocean Basin, and they attribute it to paleocirculation changes related to the separation of Australia from East Antarctica and to glacial episodes

in Antarctica. Clearly the data from Site 322, west of the entrance to the Drake Passage, bear directly on the problem of the initiation of the early circumpolar current.

The history of continental glaciation in Antarctica should both affect and be recorded by the sediments in the adjacent ocean. Evidence for Tertiary glaciation in the Jones Mountains (74°S , 94°W) was first reported by Craddock et al. (1964) and later summarized by Rutherford et al. (1972). LeMasurier (1972) described the volcanic history of Marie Byrd Land and suggested the existence of a West Antarctic ice sheet since the Eocene.

Margolis and Kennett (1970) studied the quartz grains and foraminifers in 18 cores from the South Pacific and inferred Antarctic glaciation during much of the time since the Eocene, but with a warm episode in the Miocene. During DSDP Leg 28 glaciomarine sediments were found in holes in the Ross Sea, including beds as old as early Oligocene at Site 270.

Objectives

The principal objective at Site 322 was to establish the age of the oceanic crust by drilling through the thin sedimentary sequence into the basement. Other objectives were: to determine lithology, provenance, and sedimentation process of the Bellingshausen Basin accumulations; to seek evidence of Tertiary glaciation in Antarctica; to determine the biostratigraphic sequence and the paleobiogeography of this region; to obtain specimens of basement rock for studies of composition, alteration, age, and paleomagnetism; and to obtain samples of pore waters and solid phases for studies of geochemical gradients and halmyrolysis.

OPERATIONS

The ship arrived in the vicinity of Site 322 at approximately 1700 hr on 27 February 1974. At 1735 hr speed was reduced to about 7 knots, and a brief seismic reflection survey was run (Figures 5 and 6). The beacon (13.5 kHz, O.R.E.) was dropped at 1930 hr, reaching the sea floor (5026 m corrected echo sounding depth) at 2020 hr. The vessel was stabilized over the beacon at 2115 hr, and the drill string was lowered. Bottom contact was made with the drill pipe at 5036 meters below the rig floor at 1200 hr, 28 February.

Rotation (25 rpm) was needed below about 75 meters subbottom where the first core—containing an unusually stiff mixture of sand, silt, clay—was taken.

Drilling rates within the unconsolidated silts and clays of the uppermost 300 meters varied between about 4.5 and 2.5 meters per minute. Between this depth and about 475 meters subbottom drilling rates dropped to about 1.5 meters per minute in semiindurated claystone and sandstone. Drilling rates in the lower 50 meters, where igneous rock was encountered, fell to less than 0.5 meters per minute.

The hole began to fill with grains and chips of fractured rock soon after the first basalt was recovered from 513 meters subbottom (Core 11). Drilling became increasingly difficult and 250 barrels of gel-and-water mud were needed to stabilize the hole below Core 11. Progressive deterioration of the hole, poor recovery, and the press of time led to the decision to abandon Site 322. The results of coring are summarized in Table 1.

LITHOLOGY

Observations

Thirty-four meters of sediment and igneous rock (6% of drilled sequence) were recovered from the 544 meters penetrated at this site. The sediment recovered is primarily clastic sands, silts, and clays, with occurrence of diatom oozes in the top half of the hole. The sedimentary section is divided into five lithologic units, numbered from the top down. (Table 2): (1) interbedded, unconsolidated sand, silt, clay, and diatom ooze, (2) consolidated claystone, (3) a unit containing some claystone, but dominated by sandstones, (4) a thin basal unit of pelagic brown claystone, and (5) basalt described in Igneous Rock Section. The division of the first three units is somewhat artificial because it is based primarily on sediment consolidation; the low core recovery ratios in the second unit suggest that uncon-

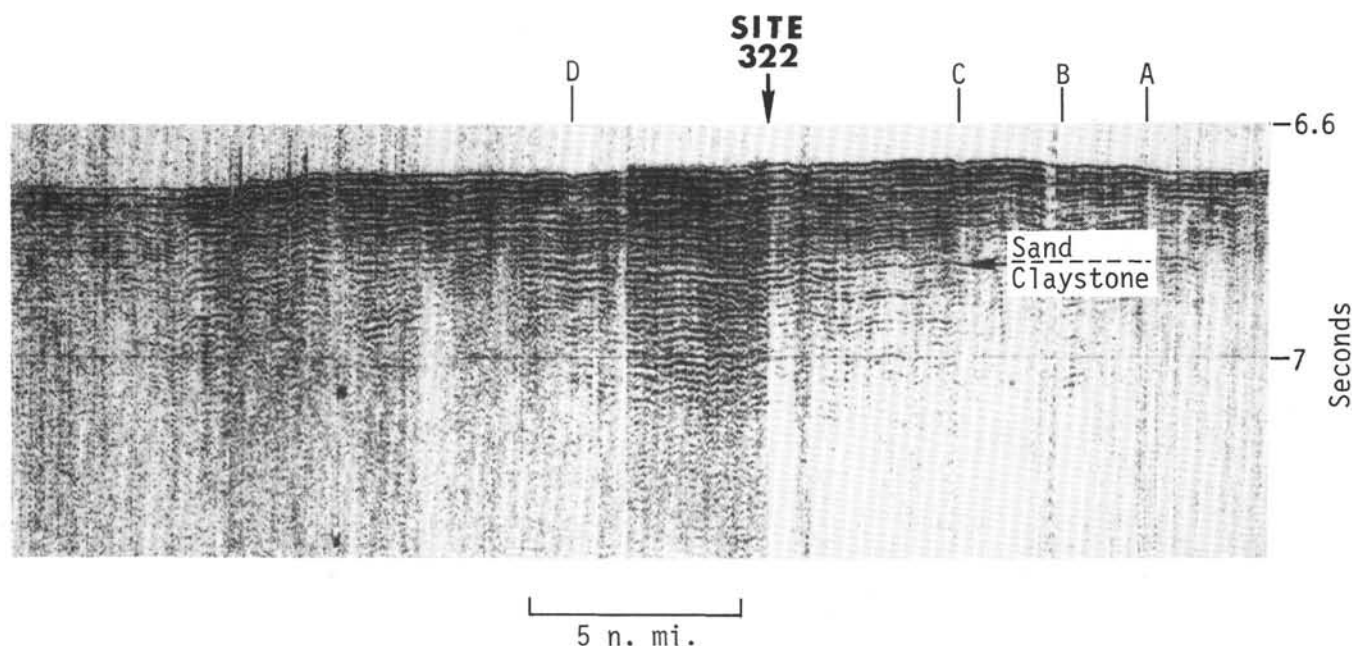


Figure 5. Glomar Challenger seismic profile approaching (A, B, C) and leaving (D) Site 322. Note lack of basement reflector. See Figure 6 for location.

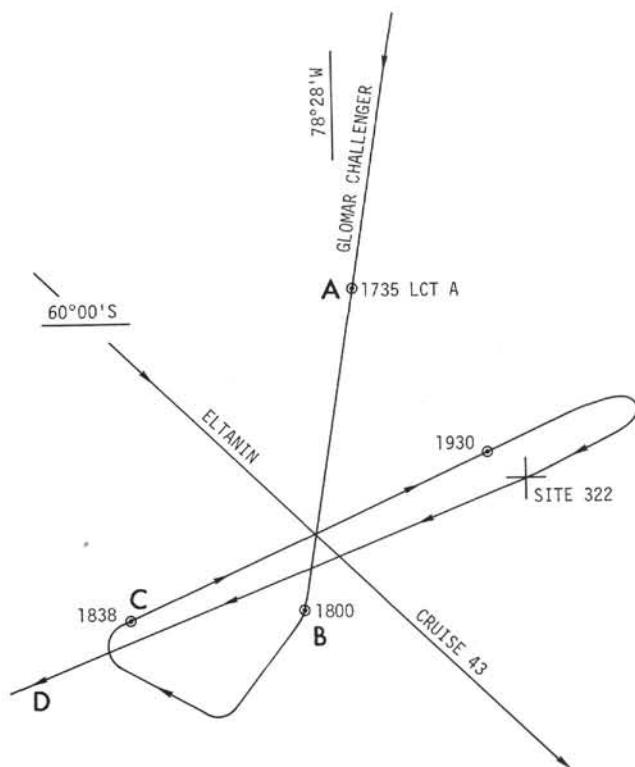


Figure 6. Glomar Challenger track approaching and departing Site 322. See also Figures 3 and 4 for Eltanin 43 seismic profile and Figure 5 for Glomar Challenger seismic profiles.

solidated sands are much more abundant at this depth than is indicated by their sparse recovery.

The base of Unit 1 is arbitrarily placed at 295 meters, just above Core 3. Cores 1 and 2 recovered greenish-gray clayey sediment with interbedded quartz sands and sandy silt beds range from mere partings to several centimeters in thickness, but show no detectable internal structure. They exhibit fair to excellent size sorting and contain fragmented diatom tests and appreciable amounts of feldspar and heavy minerals (up to 10%). Quartzose rock fragments are generally rare. Grains range from mostly angular and subangular to sub-rounded. Ice-rafted sand in the clay of Sample 3, CC (upper Miocene) is the earliest observed occurrence of ice-rafted debris at this site.

Unit 2 (Cores 3-8; 295 to 466 m) is dominated by dark greenish-gray to greenish-black claystone and silty claystone of middle (or possibly early) to late Miocene age. Cores 6-1 (438 m) and 8, CC (466 m) contain yellow-brown, crudely bedded, pelagic clays which are finely mottled and manganese stained. Quartz silt occurs locally as partings in the gray claystone but more commonly in intervals of complex, distorted laminae with admixed clay galls (disturbance is not due to coring). Feldspars and heavy minerals are usually present in quantities less than 10%, although rich heavy mineral assemblages (up to 25%) do occur. Rock fragments become common in the lower part of the unit, whereas diatoms (mostly fragmentary) persist downward in significant quantities only to Core 4 at 354 meters sub-bottom. Mineral grains are mostly angular to sub-

TABLE 1
Site 322, Coring Summary

Core	Cored Interval		Cored (m)	Recovered (m) (%)		Lithology	Age
	Total Depth (m)	Subbottom Depth (m)					
1	5112.5-5122.0	76.5-86.0	9.5	5.6	59	Sand, silt, and clay	Pliocene
2	5226.5-5236.0	190.5-200.0	9.5	2.4	25	Sand, silty clay, and clayey silt	Early Pliocene
3	5331.0-5340.5	295.0-304.5	9.5	1.2	13	Claystone	Late Miocene
4	5388.0-5397.5	352.0-361.5	9.5	2.7	28	Claystone with siltstone and sandstone	Late Miocene
5	5426.0-5435.5	390.0-399.5	9.5	1.6	17	Silty claystone	Miocene
6	5473.5-5483.0	437.5-447.0	9.5	1.7	18	Claystone and sand	Miocene
7	5483.0-4592.5	447.0-456.5	9.5	0.1	1	Quartz sand and clay pebbles	Miocene
8	5492.5-5502.0	456.5-466.0	9.5	0.2	2	Claystone	Miocene
9	5502.0-5511.5	466.0-475.5	9.5	1.9	20	Sand with some sandstone and claystone	Miocene
10	5521.0-5530.5	485.0-494.5	9.5	5.9	62	Silty sandstone and claystone	Miocene
11	5540.0-5549.5	504.0-513.5	9.5	7.9	83	Silty sandstone and claystone	Early Miocene-?Oligocene
12	5549.5-5559.0	513.5-523.0	9.5	1.2	13	Basalt cobbles	(Barren)
13	5568.5-5578.0	532.5-542.0	9.5	2.0	21	Basalt cobbles and breccia	(Barren)
14	5578.0-5580.0	542.0-544.0	2.0	0.0	0	No recovery	—
Total	5580.0	544.0	125.5	34.22	27		

Recovery of total sequence penetrated = 6%

TABLE 2
Site 322 – Summary of Lithologic Units

Unit	Lithology ^a	Subbottom Depth (m)	Unit Thickness (m)	Age
1	Gray unconsolidated sand, silt, clay, and diatom ooze	0-295	295	Holocene to late Miocene
2	Gray consolidated claystone	295-466	171	Late Miocene to middle (?early) Miocene
3	Dark gray sandstone with minor siltstone and claystone	466-509	43	Middle (?early) Miocene to early Miocene
4	Brown pelagic claystone	509-513.3	4.3	Early Miocene to (?) Oligocene
5	Basalt	513.5-542.0	>28.5	

angular, and sorting is poor to very good. The texture of a few well-sorted, unconsolidated sands may have resulted from washing during the coring process, and poor core recovery in this interval suggests the presence of significant additional quantities of unconsolidated sand.

The predominance of dark gray to gray-black sandstone in Unit 3 (Cores 9 through 11, Section 4; 466 to 509 m) distinguishes this unit from the over- and underlying units. Unit 3 ranges in age from early to middle Miocene. The lower contact with brown pelagic claystone is preserved at 54 cm in Core 11, Section 4 (509 m). The sandstone beds vary from about 1 to 5 meters in thickness and for the most part are visually uniform (massive) to very weakly bedded (at about 30° to the horizontal). The sandstones are enriched in rock fragments, quartz, feldspars, and heavy minerals, and they exhibit poor to moderate size sorting with 5%-10% clay-size material. Trace amounts of magnetite, mica, hematite, pyrite, glauconite, and recrystallized silica also appear. Contacts with interbedded claystones are sharp and usually irregular. Slight size grading occurs in the basal 20 cm of the sandstone unit bottoming in Core 11, Section 4, and the base of a similar unit in Core 10, Section 1 (490 m) contains large, angular claystone clasts of lithology similar to the underlying claystone. Faint, near-vertical stripes appear in the sandstone at the bottom of Core 11, Section 2 and top of Core 11, Section 3. They contain beautifully developed, silt-size authigenic crystals identified as analcime.

The thin (4.26 m) basal unit of the sediment column is dominantly pelagic claystone of (?) Oligocene to early Miocene age. It lies on basalt recovered in 11, CC (513.3 m), but the contact with basalt is not preserved. The uppermost claystone is dark gray, contains about 5% quartz, and is fissile (parting about 30° with horizontal) with diffuse laminae and mottles. It grades rapidly (<1 m) downward through dark greenish and olive-gray to a moderate yellow-brown claystone with only traces of terrigenous detritus. The parting in the yellow-brown claystone is horizontal, and the sediment is mottled and manganese stained. Zeolites, palagonite,

and amorphous iron oxides occur in quantities less than 5%, and the sediment is dominated by montmorillonite with significant quantities of chlorite and illite. Otherwise, the sediment is lithologically similar to the basal pelagic claystone at Site 323.

Sedimentation Processes

Turbidity Currents

The first evidence of turbidity currents at this site was seen in sediments of early Miocene age. Core 11, Section 4 at 509 meters contains a graded turbidite exhibiting several intervals of the Bouma sequence (basal graded sand, parallel laminae, and convolute laminae; Bouma, 1962). It is truncated by a thick (>4 m), dark gray, silty sandstone bed composed of rock fragments, quartz, feldspars, and heavy minerals. The bed is massive and of nearly uniform grain size, has approximately 20% matrix finer than 8 ϕ , and exhibits only slight grading in the basal 5 cm. It is noteworthy that the clayey matrix is composed of montmorillonite to the exclusion of illite, kaolinite, and chlorite (Gorbunova, this volume). The absence of more typically terrigenous clays in this otherwise terrigenous interval suggests that the montmorillonite may be the alteration product of volcanic ashes originally deposited with the sandstone. Portions of probably similar, massive sandstone beds were recovered in Cores 9 and 10. The beds locally show very faint bedding and cross-bedding but are mostly structureless.

Silty and sandy turbidites recovered commonly show a sharp, irregular basal contact on clay. The irregularity results both from erosion by turbidity currents and from postdepositional deformation (load casts). The basal parts of the turbidites contain clasts of the underlying clay which are angular to subrounded and often are deformed, indicating their original plasticity. In Sections 4-1, 4-2, and 10-1, the size of the clasts exceeds the diameter of the core; in Core 4 the structure suggests deposition of a thick bed of fluid silts which subsequently penetrated and disturbed the underlying soft clays. Strong, irregular deformation of bedding in the silts is apparent in these instances.

Core 5 (390-399.5 m) contains a remarkable bed of silty claystone which is heavily peppered with tiny (1-2 mm) clay clasts. These clasts are angular to (mostly) rounded and are oriented with their long axes horizontal, apparently being flattened by postdepositional compaction. They comprise an average of 50% of the sediment and form several weakly graded rhythmic sets. Occasional larger and irregular clay clasts (several centimeters) are scattered in this matrix. The original softness of the tiny clay clasts (indicated by their rounding during transport and by postdepositional flattening) and the presence of erratic larger clasts suggests that they were transported only a short distance; longer transport in a turbidity current would have destroyed the small clasts and cannot account for the scattered appearance of the larger clasts. It is likely that this sedimentary sequence represents deposition from a slump which originated on one of the adjacent (now buried) basement peaks.

Contour Currents

There is little evidence in the megascopic and microscopic lithology of the dominantly greenish-gray, terrigenous sediments at this site to indicate bottom current activity. This is not surprising in view of the poor core recovery and strong coring disturbance in unconsolidated sediments (Cores 1-3). Intermittent current-reworking of detritus which was initially deposited by other mechanisms is inferred from the following data:

1) Thin unstructured layers (<1 cm) and partings of silt are present in silty clay and claystone units (Cores 1 and ?4). These features are not common, but they generally exhibit sharp top and bottom contacts. Compositionally, they are dominated by quartz, heavy minerals, feldspars, and diatoms, and they exhibit moderate to excellent sorting. This latter characteristic is interpreted to result from winnowing by bottom currents. It is debatable whether these placers result from winnowing of the adjacent silty clays or from winnowing of thin silty turbidites, because the silt fraction is compositionally similar for both. However, the intensity of reworking by currents does not appear to be strong because the mineral grains are mostly angular to subangular. Although the diatoms are generally fragmentary, the angularity of the mineral grains suggests the diatoms were broken mostly during the original depositional process rather than by current reworking.

2) Core 1 also contains short intervals (<5 cm) of laminated silt-clay interbeds of less than 2 mm thick. The silts are texturally and compositionally similar to those described above, and the interbeds are therefore thought to result from winnowing by currents of variable intensity.

No erosional unconformities were detected visually in the cores recovered, but undetected hiatuses may well exist in the sparsely sampled sedimentary section.

The role that bottom currents may have played in the erosion, transportation, and deposition of clay-size material is open to question. Indirect evidence is provided by the scarcity of burrow mottling in the clays and claystones of Cores 1-9, in that sediment redistribution by bottom currents may have obscured trace

fossils. Yellow-brown claystones with only minor terrigenous silt occur sporadically in these cores; they appear to represent dominantly pelagic deposition and offer additional evidence that bottom-current activity was intermittent. The basal, yellow-brown claystone unit immediately above basalt (Unit 4) also suggests dominantly pelagic deposition; however, the presence of chlorite and illite in the unit indicates probable transportation of terrigenous clays to the site by surface currents or weak bottom currents in the (?) Oligocene to early Miocene.

It is noteworthy that some samples are well-sorted siltstones with little fine matrix; they may be current-deposited contourites or placers (Hollister and Heezen, 1972).

Interpretation

The analysis of sand layers at Site 322 indicates significant differences in the sands deposited during the Pliocene (Unit 1) and those deposited earlier during the Miocene (Unit 3). The details of the sediment composition are presented in Figure 7; a summary of the significant features is indicated below:

Unit 1	Unit 3
Size-sorting moderate to very good	Size sorting poor to moderate
Few rock fragments (some relics)	Numerous quartzose rock frags.
Quartz/feldspar >1	Quartz/feldspar \approx 1
Common diatoms and spicules	Very rare diatoms and spicules
No volcanic glass	Trace, acid volcanic glass

The sands of Unit 1 are clearly mature and may have undergone two or more cycles of transportation and deposition. The feldspars and rock fragments have been largely destroyed, and the presence of shallow water diatoms indicates a source in less than 1000 meters of water. The combined evidence strongly indicates the shelf/slope environment as the source area for these sediments.

The sands of Unit 3, containing abundant feldspar and rock fragments, are immature and were probably deposited after only one major transportation cycle. It therefore appears reasonable that these sands were derived directly from a continental source without significant residence in the shelf/slope environment.

GEOCHEMISTRY

In the upper Pliocene/Pleistocene sediment, there occurs a release of Ca^{++} and simultaneous decrease in Mg^{++} , possibly related to alteration of terrigenous debris (Peters and Hollister, this volume). Further release of Ca^{++} and uptake of Mg^{++} appear to be of importance in the lowermost sediments or in the underlying basalts. The data for dissolved potassium suggest a minor sink in the basal sediments or in the underlying basalts. Changes in the oxygen isotope composition are small, suggesting little ongoing alteration either in the sediments or in the underlying basalts (Lawrence et al., this volume).

Depletions in dissolved sulfate are small, which is also reflected in small increases in alkalinity and ammonia in the upper part of the hole. The continuous

SMEAR SLIDE SUMMARY

SITE 322



			EXOGENIC										AUTOGENIC-DIAGENETIC										BIOGENIC									
CORE	SECTION	INTERVAL cm	DETRITAL QUARTZ	FELDSPARS	HEAVY MINERALS	ROCK FRAGMENTS	LIGHT GLASS	DARK GLASS	MAGNETITE	MICA	UNIDENTIFIED OPAQUES	GLAUCONITE	CLAY MINERALS	PALAGONITE	ZEOLITES	HEMATITE	AMORPHOUS IRON OXIDES	MICRO-NODULES	PYRITE	RECRYSTALL SILICA	RECRYSTALL CALCITE	FORAM-INFERS	NANNO-FOSSILS	RADIO-LARIANS	DIATOMS	SILICO-FLAGELLATES	SPONGE	SPICULES	FISH DEBRIS	OTHER		
1	1	52							*							*									*		*					
1	1	121	*																						*		*					
1	2	29		*		*			*	*	*														*		*					
1	2	53	*		*				*		*															*		*				
1	2	73							*		*					*									*		*					
1	2	87			*				*		*														*		*					
1	2	130	*						*		*														*		*					
1	3	62		*	*																				*		*					
1	3	68																					*		*		*					
1	3	85		*	*						*													*		*		*				
1	4	47								*		*												*		*		*				
1	4	72								*						*								*		*		*				
1	6	125				*			*	*	*					*								*		*		*				
1	6	139				*			*	*	*					*								*		*		*				
1		CC				*			*	*	*	*												*		*		*				
2	2	111		*	*				*							*			*						*		*					
2	2	144		*	*				*							*									*		*					
2		CC							*	*	*														*		*					
3	1	50		*	*				*							*			*						*		*					
3	1	61.5		*	*				*	*	*					*			*						*		*					
3	1	63										*				*			*						*		*					
4	1	31		*	*						*														*		*					
4	1	32		*	*				*	*	*					*									*		*					
4	1	38.5	*													*			*						*		*					
4	1	106																	*								*					
4	1	122	*	*						*						*			*				*		*		*					
4	1	127.5		*	*			*		*						*			*						*		*					
4	2	36		*					*		*					*			*						*		*					
4	2	77		*	*		*		*	*	*					*			*						*		*					
5	1	67		*	*				*	*	*					*			*							*		*				
6	1	18		*	*		*			*	*					*			*							*		*				
6	1	32		*	*					*	*					*			*							*		*				
6	1	80		*	*		*			*	*					*			*							*		*				
6	1	145	*	*			*		*	*	*					*			*							*		*				
6		CC		*	*				*	*	*					*			*							*		*				
7		CC	*	*	*					*	*					*			*							*		*				
7		CC		*	*		*		*	*	*					*			*							*		*				
8		CC	*	*	*		*				*					*			*							*		*				
9	2	75		*	*		*			*	*					*			*						*		*					
9	2	78		*	*		*			*	*					*			*						*		*					
9		CC		*	*		*		*	*	*					*			*						*		*					
9		CC		*	*				*	*	*					*			*						*		*					
10	1	4		*	*					*	*					*			*						*		*					
10	1	17		*	*				*	*	*					*			*						*		*					
10	1	29		*	*				*	*	*					*			*						*		*					
10	1	105		*	*				*	*	*					*			*						*		*					
10	2	42		*	*		*		*	*	*					*			*						*		*					
10	5	48		*	*			*		*	*					*			*						*		*					
11	1	66		*	*		*		*	*	*					*			*						*		*					
11	2	147		*	*		*		*	*	*					*			*						*		*					
11	4	29		*	*		*		*	*	*					*			*						*		*					
11	4	32		*	*		*		*	*	*					*			*						*		*					
11	4	62		*	*		*		*	*	*					*			*						*		*					
11	4	125	*	*	*			*	*	*	*					*		*	*						*		*					
11	5	6	*	*	*				*	*	*					*	*	*	*						*		*					
11	5	19	*	*	*				*	*	*					*		*	*						*		*					
11	5	23	*	*	*				*	*	*				*	*	*	*							*		*					

Figure 7. Estimate of principal components from smear slides, Site 322.

decrease in alkalinity (and total CO_2) below 300 meters indicates the removal of carbon dioxide during the alteration processes involving the Ca^{++} increases and Mg^{++} decreases observed. Fairly high manganese concentrations indicate prevailing reducing conditions throughout the hole.

The sediments above 438 meters are generally of terrigenous origin, with the clay fraction dominated by a detrital illite/smectite, illite, and chlorite assemblage. A mineralogical break occurs below this depth as evidenced by a proportionally larger amount of illite/smectite with greater than 80% smectite layers. This material is most likely of volcanic origin. Toward the base of the section, just above the basalt, there is a progressive increase in terrigenous material, evident from an increase in illite and a decrease in illite/smectite.

The observation of an increased amount of terrigenous debris toward basalt basement is of importance. No evidence has been found for baking of the sediments, but the basal 4 meters of sediments are slightly enriched in Fe, Mn, and PO_4 . This may be due to redeposition of ridge crest material of hydrothermal origin. Underlying basalts show only minor evidence of alteration and were probably covered rapidly by sediments of both terrigenous and volcanic origin. It is not certain whether the increased contents in Fe and Mn are due to presence of ridge crest material or to enrichments in situ as a result of the alteration of volcanic material. Finally, it is possible that an actual hiatus occurs at the sediment-basalt interface. Moreover, the age of the basal section is similar to the age of the sediment overlying the unconformity at Site 323.

Data from both shipboard and shore-based geochemical investigations are presented in greater detail in the Geochemistry section of this volume.

PHYSICAL PROPERTIES

The Site 322 physical property data, which were collected at sea, are summarized in Table 3. Methods used to obtain the physical property data are discussed in detail in a succeeding chapter by Tucholke, Edgar, and Boyce.

At this site water content is highest in samples at 76-80, 193, and 295 meters. These samples are diatomaceous clays, and it is apparent that the open test structure of the interspersed diatoms has considerably increased void space in this sediment compared to non-diatomaceous clays. The effect of diatoms in increasing the porosity, and consequently the water content, of Bellingshausen Basin sediments is especially apparent when values from all four drill sites are considered.

The nondiatomaceous claystones at Site 322 exhibit a slight decrease in water content with depth and have values of 18% to 22% just above basalt (Figure 8). The water content of three sandstone samples in the lower 50 meters of the sediment column is comparable to that of the claystones.

Measured sonic velocities show a regular increase from 1.55 km/sec at 80 meters to a median of about 2.0 km/sec at 510 meters (Figure 8). The sandstone velocities in all cases are higher than those of clay-

stones at comparable depths; one sandstone at 447 meters is of considerably higher velocity (2.21 km/sec) than adjacent samples. We found no evidence of authigenic cementation in the samples, indicating that the higher velocities of sandstones must be due to well-developed intergranular contact. These velocity differences may in part relate to differences in the solid-mineral velocity and to density and porosity. These observations of increasing velocity with increasing grain size are consistent with the velocity/grain size relationships discussed by Horn et al. (1968) and Hamilton (1970).

Shipboard measurements of basalt velocities range from 4.92 to 5.04 km/sec. Basalt velocities are discussed in greater detail in Christensen (this volume). The samples tested were fresh and had a low water content (0.83%) and are described by W. Venum elsewhere in this volume.

INTERPRETATION OF SEISMIC PROFILES IN VICINITY OF SITE 322

Acoustic basement as seen in profiler records is very poorly defined in the vicinity of Site 322. The basement produces no strong reflection and is best defined by the downward disappearance of any coherent reflectors, despite the strong acoustic impedance contrast across the sediment/basalt interface (Figure 8). Careful study of the full-scale *Eltanin*-43 profile, which passes within 3 km of the site, shows that acoustic basement is strongly irregular and suggests that Site 322 was drilled near the side of a deep fissure in basement (Figure 3). The sharp declivity of the basement and its poor definition as a reflector make it very difficult to pick its depth in reflection time on the *Glomar Challenger* profiler record (Figure 5). A very poorly defined reflector near 0.505 sec subbottom appears in both the *Challenger* and *Eltanin* records at the site, and it may correspond to basaltic basement. The calculated average velocity for the sediment column is 2.03 km/sec, based on this reflection time and the basement depth of 514 meters.

Two on-site sonobuoys were attempted at Site 322, but neither drifted to sufficient range for determination of sediment velocities from the wide-angle reflections. No other sonobuoy records have been taken in the immediate area, although several sonobuoy profiles were made in similar acoustic/physiographic provinces to the southwest. Although there is marked lateral velocity variation in sediments of the deep Bellingshausen Basin, the calculated figure of 2.03 km/sec at Site 322 is in general agreement with these velocities.

The amplitude of reflectors diminishes regularly with depth at Site 322. Most of this decrease can probably be attributed to signal attenuation, although the consolidation of the deeper sediments and the apparent stabilization of their physical properties may contribute to the effect. The downward decrease in reflector strength is most marked below the clay/claystone transition at about 300 meters. Most of the sediments in the Bellingshausen Basin show at least a slight decrease in amplitude of reflectors with depth, even in many areas where the shallower sediments have low reflectivity.

In addition to signal attenuation and the steepness of the sediment/basalt interface, small-scale basement

TABLE 3
Site 322 – Summary of Physical Properties

Sample (Interval in cm)	Estimated Depth (m)	GRAPE Special 2-Min. Count Sat. Bulk Density (g/cc)				Sat. Bulk Density (g/cc)	Wet Water Content (%)	Grain Density (g/cc)	Porosity (%)	Impedance (g/cm ² sec) × 10 ⁶	Lithology Remarks
		Velocity (km/sec)		Density (g/cc)							
		Beds	⊥ Beds	Beds	⊥ Beds						
1-1, 0-15	76.50					1.47 ^a	47	2.73 ^a	73 ^a	2.28 ^b	Diatom clay
1-2, 133	79.83	1.56	1.55				50				Diatom clay
1-2, 131-135	79.81						49				Diatom clay
1-2, 135-140	79.85						24				Clay clast in drill slurry
2-1, 140-150	191.90						45				Disturbed silty clay
2-2, 110-115	193.10						47				Soft diatom claystone
3-1, 30-40	295.30						47				Soft diatom claystone
3-1, 40-42	295.40										Soft diatom claystone
3-1, 47	295.47		1.64								Soft diatom claystone
3-1, 68	295.68		1.69								Soft diatom claystone
4-2, 22-24	353.72					34	Claystone				
4-2, 30-31	353.80	1.87	1.80		1.67					3.10	Claystone
4-2, 135-150	354.85					22	Claystone				
5-1, 134-136	391.34	1.74	1.74		1.78					3.20	Silty claystone
5-1, 136-137	391.36					27	Silty claystone				
6-1, 36-39	437.86	1.82		1.94		25	Soft claystone				
6-1, 134-136	438.84					22	Soft claystone				
6-1, 136-138	438.86	1.93		1.96			Soft claystone				
7, CC	447.00		2.21		2.25					5.13	Sandstone
9-2, 139-142	468.89					24	Silty sandstone				
9, CC	469.12		1.88		1.86					3.59	Sandstone
9, CC	469.05		1.87		1.86					3.57	Sandstone
9, CC	469.08	2.04	1.86								Claystone
9, CC	469.14	2.03	1.87								Claystone
10-0, 0-15	485.00					25	Disturbed clay				
10-1, 46-48	485.96					22	Silty claystone				
10-1, 49	485.99	1.88	1.79		1.71					3.15	Silty claystone
10-1, 105-107	486.55					22	Silty sandstone				
10-1, 114	486.64	2.02	1.94		1.93					3.74	Silty sandstone
11-1, 49	504.49	2.15	2.04	1.91	1.79					3.79	Silty sandstone
11-2, 51-52	506.01					18	Silty sandstone				
11-4, 10	508.60	2.24	2.09	2.07	2.03					4.33	Silty sandstone
11-4, 84	509.34	2.20									Claystone
11-4, 124-125	509.74					22	Claystone				
11-4, 135-150	509.85					18	Claystone				
11-5, 71	510.71	1.91		1.92			Claystone				
11-5, 135-150	511.35					20	Claystone				
11-6, 13	511.63	1.88	1.76	2.00	1.95					3.50	Claystone
11-6, 57-59	512.07					23	Claystone				
12-1, 75	514.25		4.92		2.66					13.28	Basalt
12-1, 104	514.54		5.04		2.68					13.71	Basalt
12-1, 104	514.54		5.02		2.67					13.65	Basalt
13-1, 45	532.95		4.93		2.66					13.36	Basalt
12-1, 45	532.95		4.94		2.67					13.39	Basalt

^aSyringe values.

^bCalculated using bulk density from 1-2, 135-140 cm.

roughness may also contribute to the poor reflectivity of the oceanic crust in this area. Rapid drilling and coring rates (12-13 m/hr) in basement, and the texture and composition of the recovered basalt, suggest that the drill penetrated a fracture pile of hyaloclastites and pillow flows, possibly interbedded with sediments (see Vennum, this volume). Such an irregular, fractured surface could cause dispersion and absorption of the acoustic signal.

Because of the widely spaced cores at this site, there are insufficient data to attempt correlation between reflectors and physical properties changes. The only conclusion that appears to be justified is that reflector amplitude diminishes in the zone of consolidated sediments below 300 meters.

IGNEOUS ROCK

Description

About 30 basalt cobbles between 2 and 5 cm in diameter were recovered from a depth of 513 to 542 meters (Unit 5). Several of the cobbles have 5-10 mm thick glassy rinds, and small fragments of black glass are common throughout the drill cuttings. The basalt-sediment contact was not recovered, and brown clay-

stone overlying the cobbles does not show effects of contact metamorphism.

Acicular plagioclase needles (0.5-1 mm) and rectangular clear glassy microphenocrysts (1-2 mm) of plagioclase are set in a fine-grained variolitic to diabasic textural groundmass. Scattered olivine microphenocrysts (0.5-1.5 mm) are completely pseudomorphed by iddingsite. Scarce amygdules (0.5 mm) are filled with light green clay minerals. Fracture surfaces are coated with red iron oxides and manganese dendrites. The glass is veined with palagonite.

Six cobbles (2-3 cm) of basaltic breccia were also recovered. They are composed of waxy light olive to moderate greenish-yellow palagonite and dark orange altered volcanic fragments set in a brownish-black glassy matrix.

Individual cobbles collectively exhibit the complete range of textures and mineralogy found in pillow basalts recovered on DSDP Leg 16 (Yeats et al., 1973) and from *Eltanin* dredge samples (Paster, 1971). Pale to deep yellow palagonite (R.I. = 1.525 ± 0.002) veins clear light brown glass (R.I. = 1.565 ± 0.002) that contains small plagioclase laths (0.1-0.25 mm). Inward from the margins the glass contains scattered dark brown to red-brown globules (0.05-0.10 mm) com-

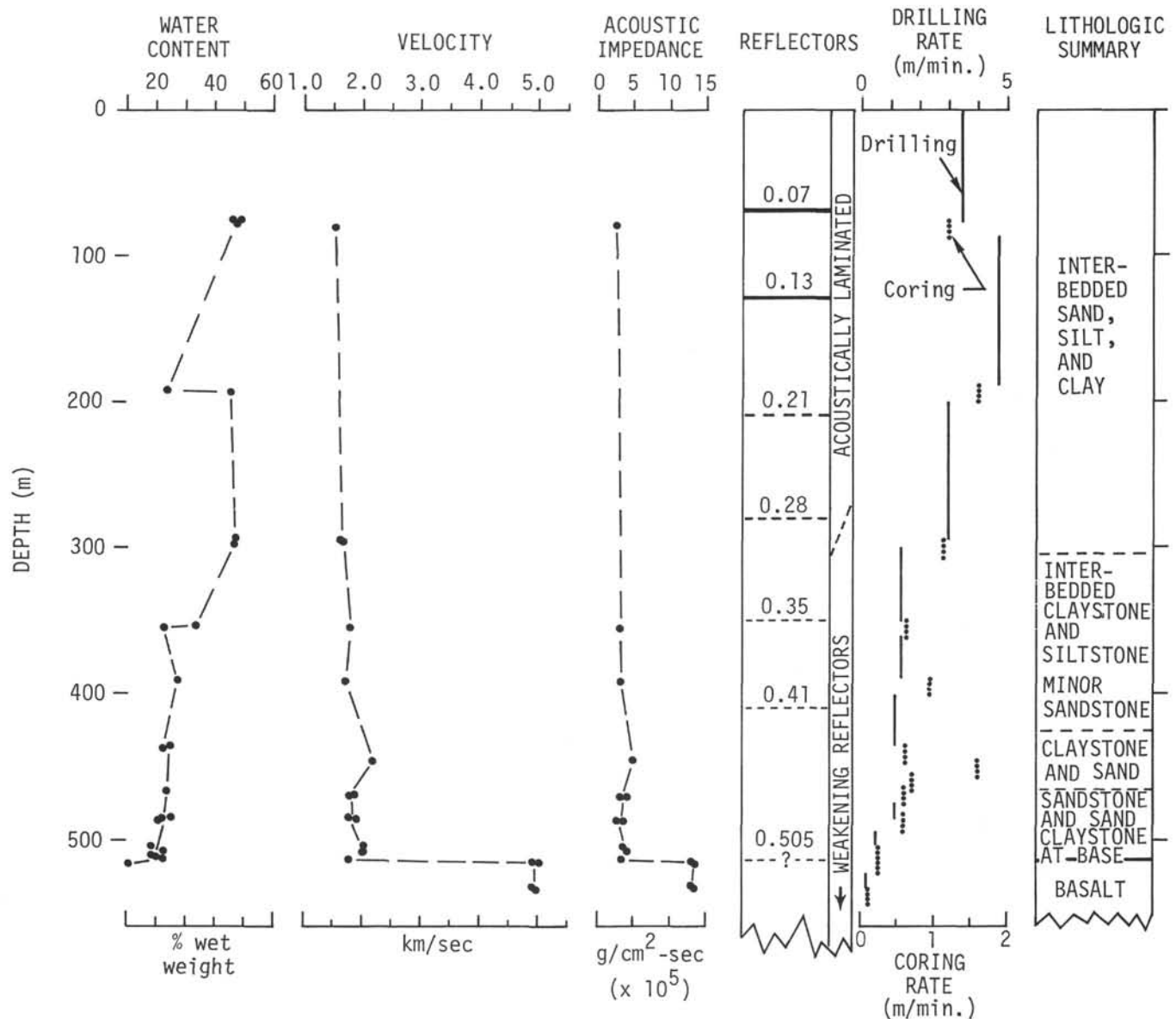


Figure 8. Summary of physical properties, acoustic character, and lithology of sediments at Site 322. Velocities are those measured perpendicular to bedding or on unoriented samples. Relative strength of reflectors is indicated by heavy solid lines (strongest) to dotted lines (weakest), and the depth of each reflector (in seconds reflection time) is indicated.

posed of radially arranged microlites. Many of these globules have nucleated about the plagioclase laths. The glass grades sharply into an opaque dark brown to dark red-brown zone composed almost entirely of polygonal globules packed so tightly that they have interfered with each others growth. Plagioclase laths in this zone have not acted as nuclei for the globules.

X-ray analysis of similar globules (Yeats et al., 1973) found in DSDP Leg 16 pillow basalts shows them to be composed of microcrystalline aggregates of plagioclase and pyroxene. Paster (1971) has traced the growth of similar globules into plumose varioles and discrete grains in basalt pillows dredged by the *Eltanin* and optically identified them as clinopyroxene. Individual cobbles from Site 322 are too small to allow tracing this gradation from glassy pillow margins to fine-grained

diabasic interior, but by examining a series of thin sections all the textural features described by Yeats and Paster can be found.

Individual cobbles with glassy rinds contain fan-shaped or plumose varioles of clinopyroxene. These varioles have not nucleated around the plagioclase, but many of the feldspar laths have "fuzzy" edges caused by the growth of incipient pyroxene microlites perpendicular to their margins. Minute grains of magnetite are concentrated along the margins of the plumose varioles, but this mineral does not occur in the outer globular zone or in the glassy margins. Scattered amygdules occur only in this variolitic zone and are filled with nonpleochroic light green clay minerals, probably iron-poor montmorillonite, that appears to be replacing microcrystalline silica (devitrified glass?).

The variolitic zone grades into very fine-grained diabasic-textured basalt. Rare euhedral olivine microphenocrysts occur in these innermost two zones and are completely pseudomorphed by iddingsite and in places veined by serpentine. Widely scattered glomeroporphyritic clots of plagioclase and pyroxene occur throughout the diabasic zone. These pyroxene crystals have the same refractive index and birefringence as groundmass pyroxene. An augitic composition is indicated by an average $2V$ of 60° . The pyroxene is fresh, colorless, shows only very slight zonation, and is not titaniferous.

Inward from the globular zone plagioclase occurs as acicular needles or as rectangular microphenocrysts. The needles have length-to-width ratios as high as 20 or 30:1 and are commonly doubly swallowtailed. They are twinned on both the albite and Carlsbad laws. Zonation is weak or absent, and their composition ranges only from An_{70} to An_{65} . The larger needles are isolated in the groundmass, but the smaller ones are commonly arranged in fan-shaped aggregates or grow from a common center like the spokes of a wheel. None is saussuritized, but some are cored with intergrown clinopyroxene needles. The microphenocrysts are fresh, essentially untwinned and only occasionally show slight oscillatory zoning. The refractive index is similar to that of the plagioclase needles. One quarter of the microphenocrysts have clinopyroxene cores, and half have sharply bounded cores of untwinned feldspar with a lower refractive index than the rims. This latter feature appears to be reverse zonation, but Bass et al. (1973) and Stewart et al. (1973) have described plagioclase with K-feldspar cores in basalts recovered during DSDP Legs 17 and 19, respectively. Compositional determinations are outlined by Vennu (this volume).

The rare occurrence of olivine phenocrysts, the absence of groundmass olivine, and the late crystallization of magnetite are suggestive of a tholeiitic composition. The breccia cobbles contain fragments of variolitic-textured basalt identical to that described above, but are composed mainly of angular fragments of glass and palagonite embedded in a glassy matrix. They are interpreted to be hyaloclastites.

Basalt cobbles obtained at Site 322 are remarkably fresh. Very thin coatings of reddish-iron oxides and manganese dendrites discolor fracture surfaces on less than half the cobbles. Veins of calcite and chlorite were not observed. Glassy rinds are veined by palagonite, but the veins are thin and much fresh glass remains. Euhedral olivine microphenocrysts completely pseudomorphed by iddingsite and amygdules filled with light green montmorillonite (?) collectively comprise less than 1% of the recovered rock. Clinopyroxene and plagioclase, which make up most of this essentially biminerallitic basalt, have not been affected by either deuteric alteration or submarine alteration. Density (2.70 - 2.72 g/cm³), H₂O content (0.76% - 0.86% by wt), and CO₂ content (0.03% - 0.6% by wt) are all indicative of fresh basalt. Sonic velocity values (4.92 - 5.04 km/sec) are relatively low for fresh basalt, but are comparable to average values for basalts recovered on previous DSDP legs. Submarine alteration of the recovered basaltic cobbles has not proceeded beyond the incipient

stages at this site. Fragments incorporated in the hyaloclastite cobbles, however, are extensively palagonitized.

Drilling and coring rates of 12 - 13 m/hr in the basalt are surprisingly high. Generally, 3 m/hr is considered fast. This suggests that the drill penetrated either a fractured pile of hyaloclastites and pillow flows or a sequence of basalt and sediment. Movement of lava beneath a cover of hyaloclastites and pillows could easily fracture this material into angular fragments. Gradation from glass through globule and variolitic zones to very fine grained, diabasic textured basalt, and the coexisting hyaloclastite argue strongly against the presence of a sill. Interlayered flows and sediments would suggest off-ridge volcanism. The apparent tholeiitic affinities of the basalt suggest origin at a mid-ocean ridge, but the freshness of the lava argues for an age consistent with the paleontological data, i.e., much younger than that expected by extrapolation of distance from the East Pacific Rise (Herron, 1971) or of depth below sea level (Sclater et al., 1971).

BIOSTRATIGRAPHY

Foraminifers

Cores 1 through 10 were barren of foraminifers except a few reworked benthonic specimens in Cores 6 to 9. Core 11, Sections 4 to 6 (Lithologic Unit 4 overlying basement) yielded a fauna of badly preserved arenaceous foraminifers. The species *Haplophragmoides carinatus*, *Cyclammina incisa*, *C. cf. japonica*, and *C. cf. rotundata* indicate an ? Oligocene to early Miocene age.

Nannoplankton

All cores are nearly devoid of calcareous nannoplankton. At a single level in Core 3 a few small nondescript placoliths were observed as contaminants.

Radiolarians

Eleven "spot" cores with a total length of 34.2 meters were recovered before basement was encountered at a subbottom depth of 513.3 meters.

Poor to moderately well preserved radiolarians of latest Paleogene (?) and Neogene age occur sporadically throughout Site 322 sediments (Table 4). Cores 1, 2, 4, 6, 8, and 9 contain radiolarian assemblages with low abundances and low species diversity. Other cores examined were either totally barren of radiolarians or contained specimens which were recrystallized.

Core 1, Section 1, 44 - 46 cm through Core 2, Section 2, 97 - 99 cm contains moderately well preserved specimens of *Desmospyris spongiosa*, *Helotholus vema*, *Eucyrtidium calvertense*, *Clathrocyclas bicornis*, *Prunopyle (?) titan*, and *Lychnocanoma grande rugosum* which are diagnostic of a Pliocene age for this interval (latest Gilbert-Gauss), and places it within the Upsilon Zone of Hays and Opdyke (1967) and the *Helotholus vema* Zone of Chen (1975).

Core 322-3 is totally barren of radiolarians, but the presence of poorly preserved specimens of *Dendrosphyris haysi*, *Eucyrtidium* sp. aff. *E. inflatum*, *Pruno-*

TABLE 4
Occurrence of Radiolarians at Site 322

Sample (Interval in cm)	Species		Abundance	Preservation	Age	Zone																																			
							<i>Antarctissa denticulata</i>	<i>A. strelkovi</i>	<i>A. conradae</i>	<i>A. antedenticulata</i>	<i>Spongostrochus glacialis</i>	<i>Spongodiscus osculosus</i>	<i>Lithelius nautiloides</i>	<i>Stylactactis neptunus</i>	<i>S. universus</i>	<i>Saccospyris antarctica</i>	<i>S. conithorax</i>	<i>Siphocampe aquilonaris</i>	<i>Lithomitra arachnea</i>	<i>Cornutella profunda</i>	<i>Cyrtopera languncula</i>	<i>Collosphaeridae</i>	<i>Prunopyle terapila</i>	<i>Pterocorys hirundo</i>	<i>Peripyramis circumtexta</i>	<i>Desmospyris spongiosa</i>	<i>Helotholus vema</i>	<i>Clathrocyclas bicornis</i>	<i>Eucyrtidium calvertense</i>	<i>E. cienkowskii</i> group	<i>E. inflatum</i> (?)	<i>Lychnocanoma grande rugosum</i>	<i>Prunopyle titan</i>	<i>Dendrospyris haysi</i>	<i>Prunopyle haysi</i>	<i>Actinomma tanyacantha</i>	<i>Stichocorys peregrina</i> (?)	<i>Orosphaeridae</i>	<i>Theocorys redoensis</i>		
322-1-1, 44-46	C	M					C	F	-	-	C	F	R	F	-	R	-	R	R	R	-	-	R	-	-	-	C	-	R	C	-	-	-	-	-	-	-	-	-	R	
322-1-2, 64-66	-	-																																							
322-1-3, 19-21	F	M					R	R	-	R	F	F	-	-	-	R	R	R	-	-	-	-	-	-	-	-	-	-	R	C	-	-	-	-	-	-	-	-	-	-	
322-1-4, 70-72	C	M					C	C	-	-	C	-	R	R	-	R	-	-	-	-	-	-	-	-	-	-	-	-	-	C	-	-	-	-	-	-	-	-	-	-	-
322-1, CC	F	M					F	R	-	F	F	R	-	-	-	R	-	-	-	R	-	+	-	-	-	-	R	R	-	-	F	-	R	R	-	-	-	-	-	-	-
322-2, 97-99	C	G					F	R	+	F	F	F	R	-	-	R	-	-	-	R	-	-	-	-	-	-	-	C	-	-	-	-	-	-	-	-	-	-	-	-	-
322-2, CC	F	M					-	-	-	+	-	+	-	-	-	-	-	-	-	-	-	-	-	-	-	-	-	-	-	F	-	R	-	-	-	-	+	+	-	-	-
322-3-1, 46-48	-	-																																							
322-3, CC	-	-																																							
322-4-1, 73-75	R	P					-	-	-	-	-	-	-	-	-	-	-	-	-	-	-	-	-	-	-	-	-	-	-	-	-	-	-	-	-	-	-	-	-	-	-
322-4, CC	R	P					-	-	-	-	-	-	R	-	R	-	-	-	-	-	-	-	-	-	-	-	-	-	-	R	-	R	-	-	-	R	R	-	-	-	-
322-5-1, 98-100	-	-																																							
322-5, CC	-	-																																							
322-6-1, 84-86	-	-																																							
322-6, CC	F	P																																							
322-7, CC	-	-																																							
322-8, CC	F	M					-	-	-	-	-	-	-	-	-	-	-	-	-	-	-	-	-	-	-	-	-	-	-	-	-	-	-	-	-	-	-	-	-	-	
322-9-2, 75-82	F	P					-	-	-	-	-	-	-	-	-	-	-	-	-	-	-	-	-	-	-	-	-	-	-	-	F	-	-	-	-	-	-	-	-	-	
322-9, CC (Top)	F	P					-	-	-	-	-	R	-	-	-	-	-	-	-	-	-	-	-	-	-	-	-	-	-	R	-	-	-	-	-	-	-	-	-	-	
322-9, CC (Bottom)	-	-																																							
322-10-2, 41-43	-	-																																							
322-10-6, 130-132	-	-																																							
322-10, CC	-	-																																							

pyle haysi, *Stichocorys* (?) *peregrina*, *Eucyrtidium calvertense*, and *Actinomma tanyacantha* in Samples 322-2, CC and 4, CC is diagnostic of a late Miocene age. No biostratigraphic zonal definition of this interval was possible due to the absence of any of the index species proposed by Chen (1975).

The only radiolarians identified between Cores 5 through 10 occur in three samples, 322-8, CC, 322-9-2, 75-82 cm, and 322-9, CC (top). These are dated as Miocene on the basis of the occurrence of *Dendrosphyris haysi*, *Eucyrtidium calvertense*, and *E. cienkowskii* group. Cores 322-5, 7, and 10 are totally barren, but Core 322-6 does contain some recrystallized specimens of the *E. cienkowskii* group.

Silicoflagellates

Silicoflagellates were found in only the upper 4 of the 10 cores recovered at Site 322. Core 1, Section 1 contains several specimens of fairly well preserved *Distephanus speculum* (short-spined variety) along with rare occurrences of *Dictyocha fibula*. Section 2 of Core 1 also contains several short-spined *D. speculum*, but in contrast to Section 1, several well-preserved specimens of *Mesocena diodon* were also present. *Distephanus*

boliviensis occurs only rarely and was found in the core-catcher sample of Core 1. These species indicate a late Miocene-early Pliocene age for Core 1, Section 2.

Samples examined from the core-catcher samples of Cores 2, 3, and 4 contain *Mesocena diodon* and/or *Mesocena circulus*. Both species indicate a possible late Miocene age for these cores.

Diatoms

The youngest sediment recovered at Site 322 (322-1-1, 79-80 cm) falls into the *Nitzschia interfrigidaria* Zone of McCollum (1975), on the basis of common *Nitzschia interfrigidaria*, *Cosmiodiscus insignis*, and *Coscinodiscus lentiginosus*. This zone has been correlated to the paleomagnetic stratigraphy and is 2.8-3.65 m.y.B.P. Samples 322-1-2, 61-62 cm through 322-2-2, 141-142 cm are placed into the *Nitzschia interfrigidaria*-*Nitzschia praeinterfrigidaria* zones of McCollum (1975) on the basis of the occurrence of *Cosmiodiscus insignis*. No individuals of *Nitzschia praeinterfrigidaria* or *N. interfrigidaria*, however, were found. The age of this interval is 3.65-3.82 m.y.B.P. Samples 2, CC through 4, CC contained only a poorly preserved diatom assemblage. *Denticula hustedtii* and

Trinacria excavata are common and the interval is placed into the *Denticula hustedtii* Zone of McCollum (1975) which is lowermost Pliocene to late Miocene in age.

RATES OF SEDIMENT ACCUMULATION

The average accumulation rate for the upper 75 meters of sediment at Site 322 is calculated to be between 2 and 3 cm/1000 yr (Figure 9). This calculation is based on a Pliocene date indicated by radiolarian and diatom zonation from Core 1. The average accumulation rate increases sharply to 10 to 12 cm/1000 yr below Core 1 down to a depth of about 360 meters (Core 4). These accumulation rates are much higher than the rate of 0.4-0.5 cm/1000 yr determined by Goodell and Watkins (1968) for the Brunhes (Pleistocene) age sediments recovered in piston cores in this area. The discrepancy is apparently related to either (1) less intense scour of Pliocene to Pleistocene age sediments by bottom currents, or (2) greater local influx of terrigenous detritus during this period (see also Lithology, this chapter).

The age of Core 11 at the bottom of the sedimentary sequence is (?) Oligocene to early Miocene as indicated by the presence of arenaceous forams, particularly the genus *Cyclammina*. Cores between 5 and 11 did not yield paleontological ages so only an average sediment accumulation rate of 1 to 1.5 cm/1000 yr can be calculated for sediment below 360 meters at Site 322.

SUMMARY AND CONCLUSIONS

Summary

Site 322 is located on the Bellingshausen Abyssal Plain at a water depth of 5026 meters. The one hole drilled at this site reached a total depth of 544 meters, penetrating 31 meters into basaltic rock at the bottom. The upper 513 meters consist of Neogene sedimentary deposits. A total of 125.5 meters was cored; 34.2 meters (27%) of core were recovered. A graphic summary of coring results is presented in Figure 10.

Five lithologic units are recognized, four sedimentary and one igneous; these units are numbered in descending order. Unit 1 is about 295 meters thick and consists of unconsolidated, well-sorted sands and silts interbedded with clays, with upper Miocene ice-rafted debris. Quartz is more abundant than feldspar in the sands, and few rock fragments and no volcanic glass fragments were observed. Diatoms and sponge spicules are common. The basal contact occurs in the interval between Core 2 and Core 3, but it was not preserved in the recovered core.

Unit 2 is about 171 meters thick and consists of dark gray consolidated claystone. Quartz silt is abundant in some beds, and feldspar grains, heavy minerals, and diatom fragments are minor components. Neither the upper nor lower contacts are preserved in the cores.

Unit 3 is about 43 meters thick and consists of interbedded, mainly dark gray sandstones and claystones. The sandstones are poorly to moderately sorted and contain many rock fragments and some vol-

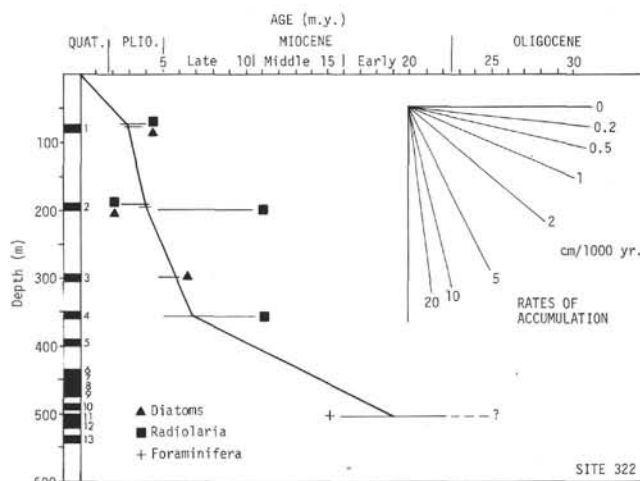


Figure 9. Rate of sediment accumulation, Site 322.

canic glass fragments; feldspar is about as abundant as quartz. Diatoms and sponge spicules are rare.

Unit 4, of early Miocene to ?Oligocene age, is 4.3 meters thick, and arenaceous foraminifers are present in the distinctive yellowish-brown claystone at the base of this unit. Neither the upper nor lower contacts are preserved in the cores. Cuttings of claystone from just above the underlying basalt are dense, hard and shiny, but they do not appear to be baked.

Unit 5 is at least 30 meters thick and consists of holocrystalline, variolitic, and glassy basalt. Rock recovered in this unit is in the form of numerous small chips and about 30 moderately rounded pebbles and cobbles. Some cobbles have glassy rims, and small fragments of black glass are common in the drill cuttings. Scarce amygdulites are filled with a light green mineral, and fracture surfaces are coated with red iron oxides and manganese dendrites. Six cobbles of breccia with a glassy matrix are interpreted as hyaloclastites. Although some of the glass is cut by small palagonite veins, most of these igneous rocks appear fresh and unaltered. The curved glassy rims on some cobbles are interpreted as parts of lava pillows. Measured sonic velocities range from 4.92 to 5.04 km/sec, and measured densities from 2.66 to 2.68 g/cm³.

Seismic profiles at the site show a series of horizontal to gently undulating reflectors which become less coherent downward. No definite correlations could be established between individual reflectors and lithologic contacts within the sedimentary sequence. Although measured sonic velocity increases abruptly from 1.76 to about 5.00 km/sec, the sedimentary-igneous contact cannot be seen on the seismic profile. This contact occurs, however, at about the depth on the profiles where coherent reflectors disappear.

The sedimentary sequence is impoverished in fossils, and many core sections appear to be barren. Diatoms are the most abundant forms, and they are common in some beds of Units 1 and 2; species diversity, however, is low. Displaced shallow-water marine benthonic species are common in some beds of Unit 1. The youngest recovered diatoms are placed in the *Nitzschia interfrigidaria* Zone of Pliocene age.

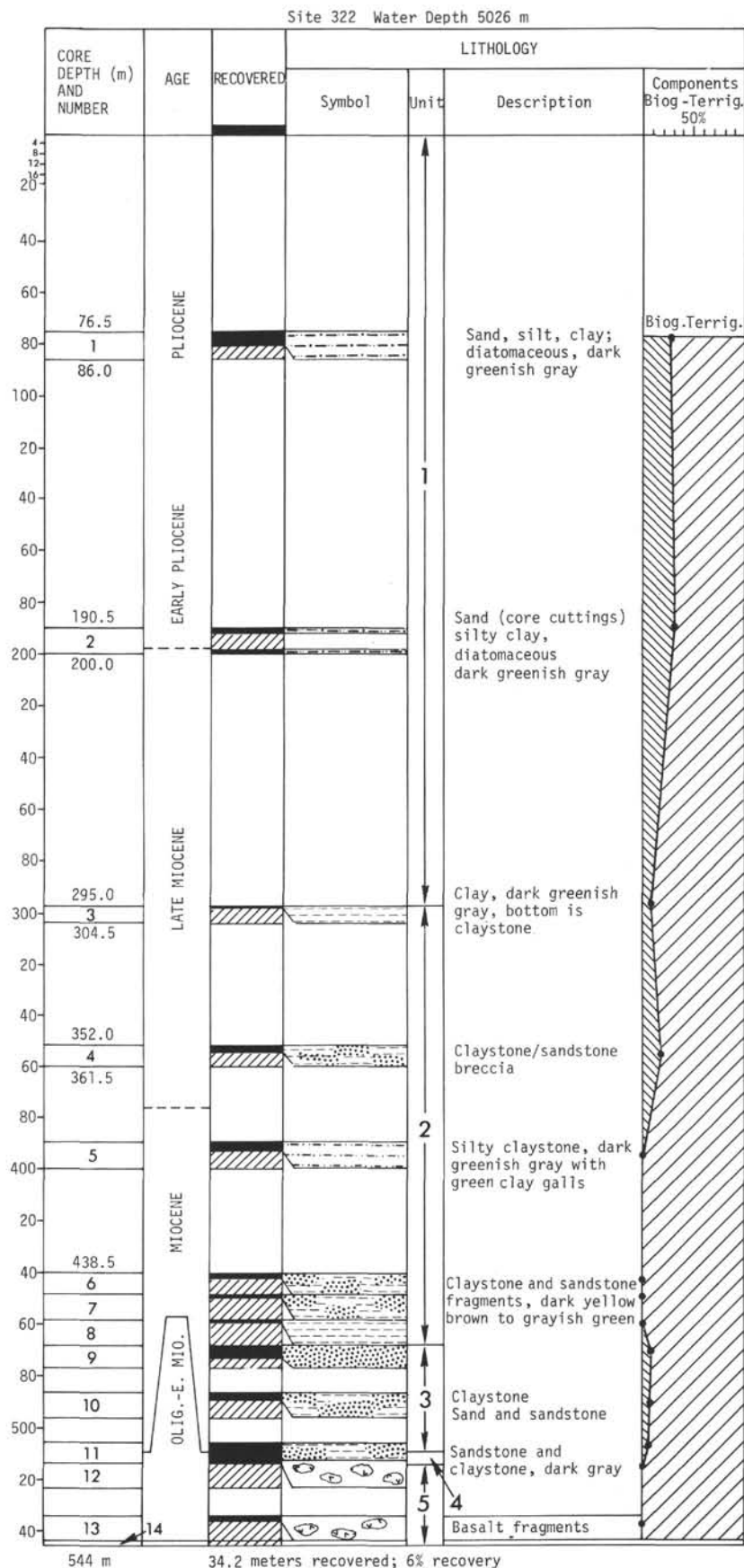


Figure 10. Lithologic and biostratigraphic summary, Site 322.

Latitude 60°01.45'S Longitude 79°25.49'W

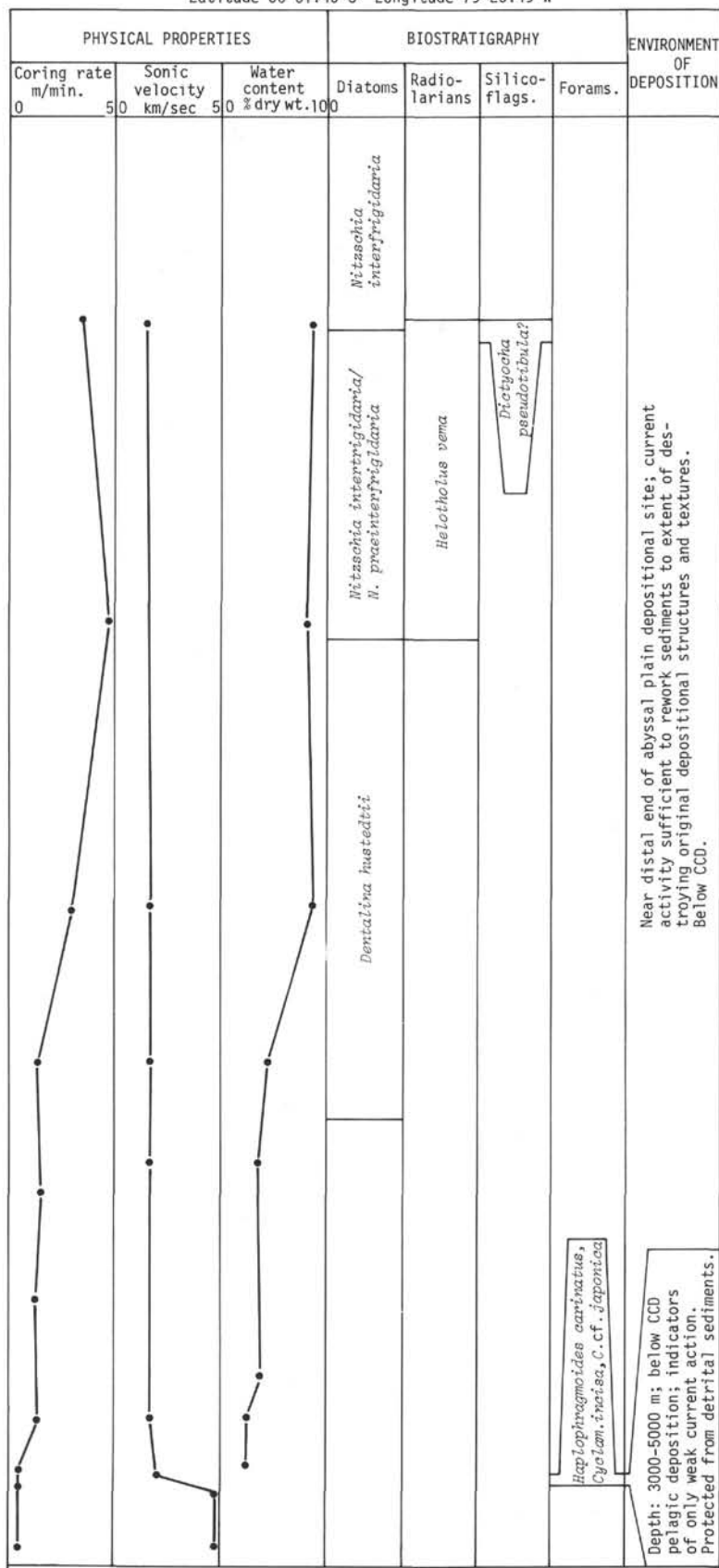


Figure 10. (Continued).

Other fossil groups are scarce in the sedimentary sequence. Pliocene radiolarians occur in the first core, but they become rare and less diagnostic deeper in the hole. A few silicoflagellates found in Unit 1 and the upper half of Unit 2 yielded ages increasing downward from late Pliocene to late Miocene. Several benthonic arenaceous foraminifers (*Bathysiphon*, *Ammodiscus*, and *Cyclammina*) were found in claystone of Units 3 or 4 within a few meters of the basalt contact; they indicate an early Miocene to ? Oligocene age. All cores are barren of nannoplankton.

Twelve interstitial water samples were taken from the sedimentary sequence for shipboard and shore-laboratory geochemical studies. Downhole increases in formation factor, pH, and dissolved calcium were observed, along with decreases in water content (%), alkalinity, and dissolved silica and magnesium. Dissolved ammonia increases to a maximum near 200 meters in the hole, and from there decreases downhole.

Conclusions

The oldest rock penetrated at Site 322 is the basalt in the lowest 30 meters of the hole. On the basis of amygdules, glassy veins on inferred pillows, and hyaloclastite breccia, this rock is interpreted as a submarine lava flow. If the overlying claystone, which contains arenaceous benthonic foraminifers of bathyal to abyssal type, is conformable, then the eruption occurred in "deep" water relative to the mid-Tertiary calcium carbonate compensation depth. The basaltic rock is generally quite fresh, but the flat surfaces coated with iron and manganese minerals indicate the presence of fractures. The poor core recovery and the high penetration rate (12-13 m/hr) suggest that this interval may consist of interbedded thin lava flows and sediments.

The age of the basaltic extrusive rock can only be approximated. Microfossils from the overlying sedimentary sequence indicate that the basaltic rock, if indeed extrusive, can be no younger than early Miocene. If an unconformity separates the basalt and the overlying sedimentary sequence, a significantly older age for the igneous rock is possible. The presence of glass in the basaltic rock, some quite fresh in appearance, suggests a Cenozoic age; a Cretaceous age, however, is not precluded.

It is not clear whether this igneous rock represents crustal basement, or whether older sedimentary beds may underlie it.

Several interpretations are possible: (1) the basalts are middle Tertiary and represent a random sea-floor eruption; (2) the basalts are middle Tertiary in age and may represent true igneous basement; (3) the basalts represent true basement and may be as old as Cretaceous, the lack of pre-middle Tertiary sediments overlying the basalt being due to erosion by bottom currents which diminished by Miocene time. The presence of fresh glass suggests a Cenozoic age but several factors support the basement interpretation: (1) lithologic and chemical similarity to other DSDP basalts interpreted to be true basement; (2) absence of deeper reflectors in seismic profiles of the area; (3) lateral continuity of acoustical basement beneath most

of the abyssal plain. The problem of finding a nearby spreading axis source for a middle Tertiary basement is still unsolved. K-Ar dates obtained from Site 322 (10-15 m.y.B.P.) are geologically unrealistic.

The observed geochemical gradients in the interstitial waters suggest that halmyrolysis has occurred, but these gradients are compatible with each of the above models.

The position of the site on the abyssal plain and the southward continuity of stratigraphic units in the seismic profiles indicate that most of the detritus in the sedimentary sequence came from Antarctica. The sands of Unit 1 are mature, but the older sands of Unit 3 are immature. The scarcity of sedimentary features common in turbidites suggests that bottom currents were the agent for the final deposition of many of these sediments. Only a few ice-rafted clasts were observed in the limited core recovered, but their scarcity is not surprising in view of the high sedimentation rate and the distance from Antarctica (700 miles).

The average accumulation rate for the upper 100 meters of beds, based on a good date from diatoms and radiolarians, is about 2 cm/1000 yr. An even greater rate of 10 to 12 cm/1000 yr is tentatively suggested for the 100-350 meter sequence in the hole. The average accumulation rate calculated for sediments below 350 meters is between 1 and 1.5 cm/1000 yr.

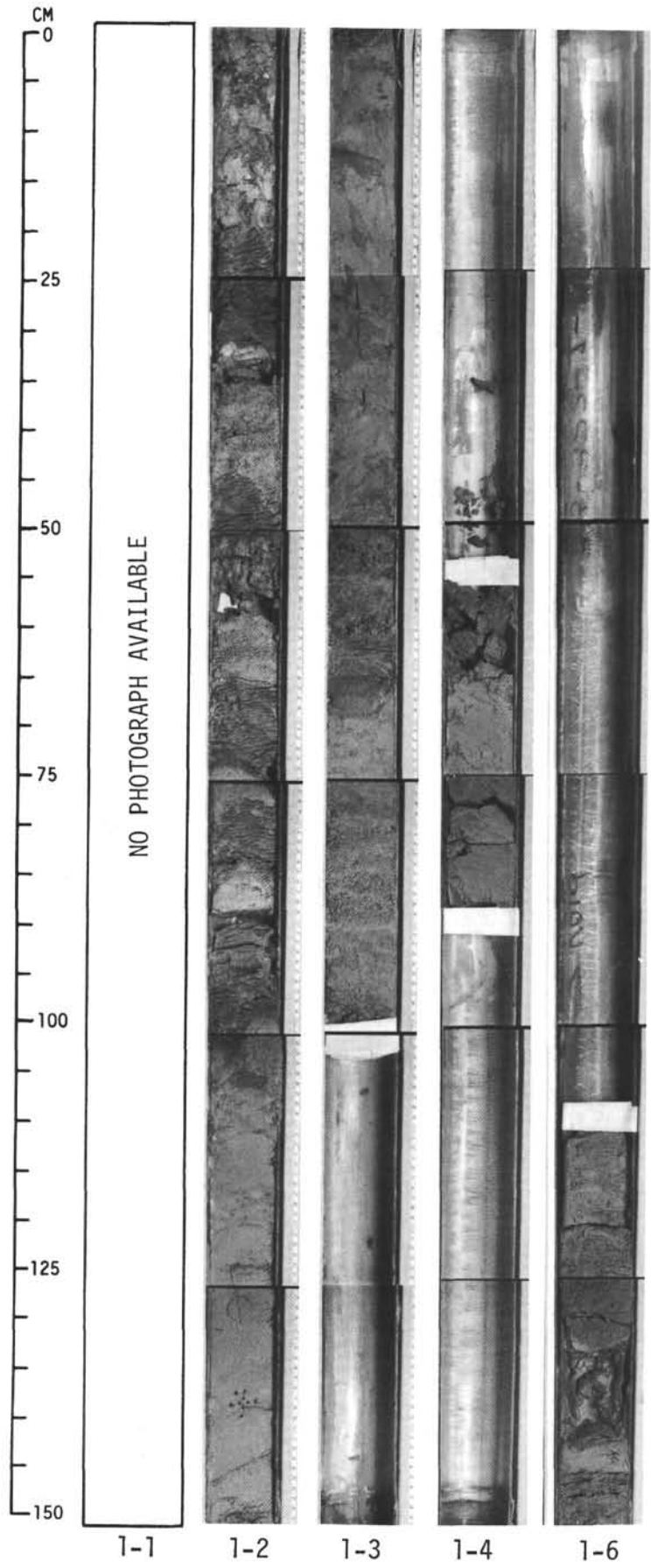
The scarcity of fossils in the deeper cores from this site probably results from extensive dissolution of tests rather than from limited populations in these seas during the Cenozoic. Most or all of the sedimentary sequence is Neogene in age, but an age as old as Oligocene remains a possibility for the oldest beds.

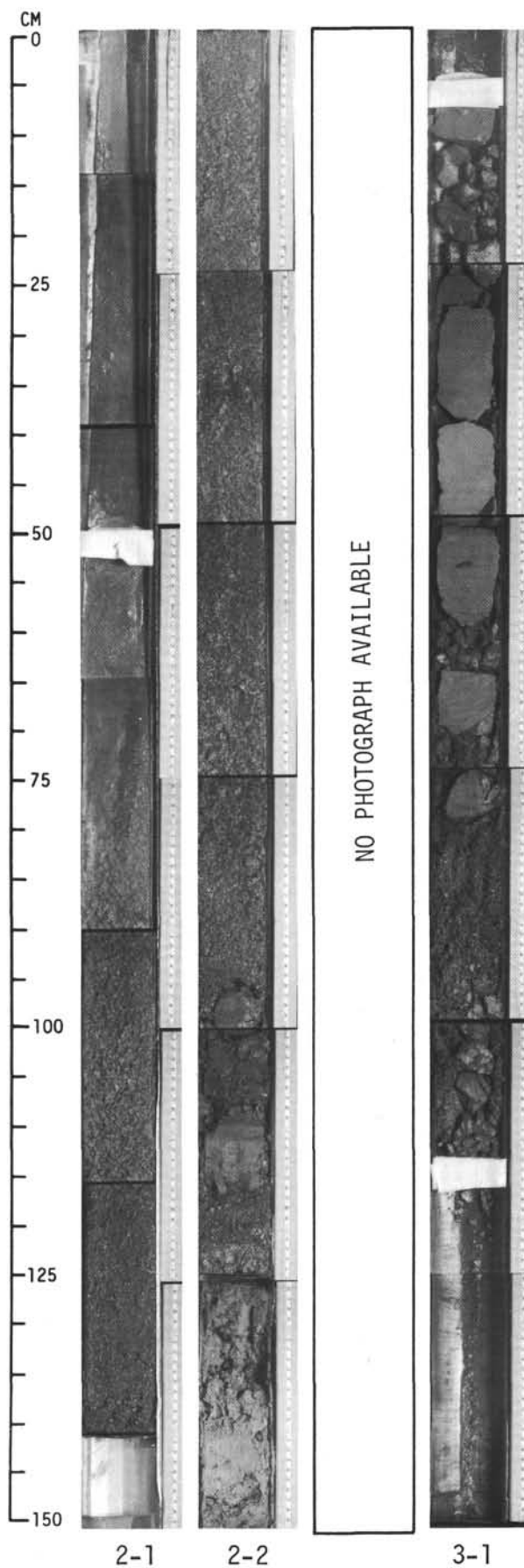
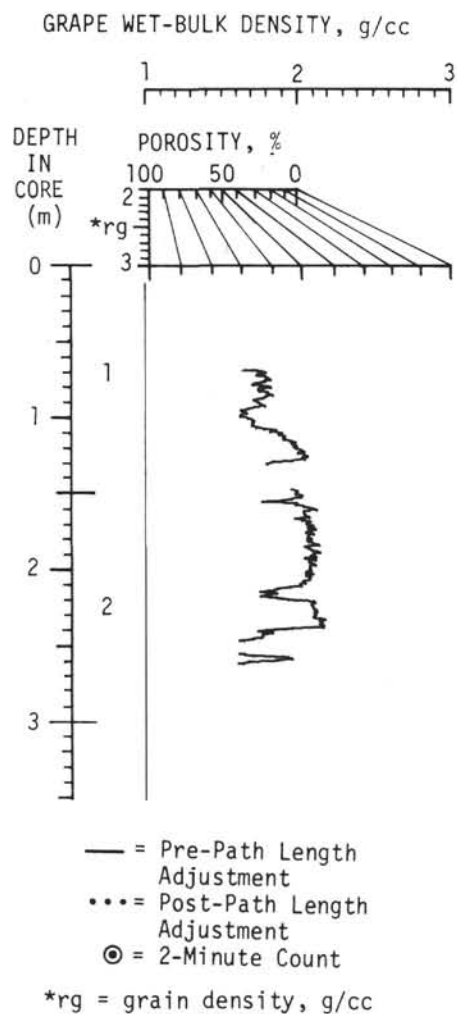
REFERENCES

- Adie, R.J., 1970. Antarctic Peninsula. In *Geologic maps of Antarctica Folio 12*, Antarctic Map Folio Series: New York (Am. Geogr. Soc.).
- Bass, M.A., Moberly, R., Rhodes, J.M., Shih, C., and Church, S.E., 1973. Volcanic rocks cored in the central Pacific, Leg 17. In *Winterer, E.L., Ewing, J.L., et al., Initial Reports of the Deep Sea Drilling Project, Volume 17*: Washington (U.S. Government Printing Office), p. 429-504.
- Bouma, A.H., 1962. *Sedimentology of some physch deposits*: Amsterdam (Elsevier).
- Boyce, R.E., 1973a. DSDP density-porosity parameters and their determinations by gravimetric and GRAPE techniques: Unpublished DSDP manual.
- Boyce, R.E., 1973b. Physical properties—methods. In *Edgar, N.T., Saunders, J.B., et al., Initial Reports of the Deep Sea Drilling Project, Volume 15*: Washington (U.S. Government Printing Office), p. 1115-1127.
- Chen, P., 1975. Antarctic Radiolaria, Leg 28, Deep Sea Drilling Project. In *Frakes, L.A., Hayes, D.E., et al., Initial Reports of the Deep Sea Drilling Project, Volume 28*: Washington (U.S. Government Printing Office), p. 437-513.
- Craddock, C., 1972. Geologic map of Antarctica, scale 1:5,000,000: New York (Am. Geogr. Soc.).
- , 1975. Tectonic evolution of the Pacific margin of Gondwanaland. In *Campbell, K.S.W. (Ed.), Gondwana*

- Geology: Canberra (Australian National University Press), p. 609-618.
- Craddock, C., Bastien, T.W., and Rutford, R.H., 1964. Geology of the Jones Mountains. In Adie, R.J. (Ed.), *Antarctic geology*: Amsterdam (North Holland Publ. Co.), p. 171-187.
- Dalziel, I.W.D. and Elliot, D.H., 1973. Scotia Arc and Antarctic margin. In Nairn, A.E.M. and Stehli, F.G. (Eds.), *The Ocean basins and margins*, vol. 1: New York (Plenum Publ. Corp.), p. 171-246.
- Gansser, A., 1973a. Facts and theories on the Andes: *J. Geol. Soc. London*, v. 129, p. 93-131.
- , 1973b. Orogene Entwicklung in den Anden, im Himalaja und den Alpen, ein Vergleich: *Ecolog. Geol. Helv.*, v. 66, p. 23-40.
- Gonzalez-Ferran, O., 1972. Distribución del volcanismo activo de Chile y la reciente erupción del volcán Villarrica: In *El Primer Symposium Cartográfico Nacional*, Santiago, p. 191-207.
- Goodell, H.G., Houtz, R., Ewing, M., Hayes, D., Naini, B., Echols, R.J., Kennett, J.P., and Donahue, J.G., 1973. Marine sediments of the southern oceans, Folio 17, Antarctic Map Folio Series: New York (Am. Geogr. Soc.).
- Goodell, H.G. and Watkins, N.D., 1968. The paleomagnetic stratigraphy of the Southern Ocean: 20° west to 160° east longitude: *Deep-Sea Res.*, v. 15, p. 89-112.
- Gordon, A.L., 1967. Structure of Antarctic waters between 20° W and 170° W, Folio 6, Antarctic Map Folio Series: New York (Am. Geogr. Soc.).
- , 1972. On the interaction of the Antarctic circumpolar current and the Macquarie Ridge. In *Antarctic Oceanology II*, Antarctic Res. Ser.: Am. Geophys. Union, p. 71-78.
- Griffiths, D.H. and Barker, P.F., 1972. Review of marine geophysical investigations in the Scotia Sea. In Adie, R.J. (Ed.), *Antarctic geology and geophysics*: Oslo (Universitetsforlaget), p. 3-11.
- Hamilton, E.L., 1970. Sound velocity and related properties of marine sediments, North Pacific: *J. Geophys. Res.*, v. 75, p. 4423-4445.
- Hays, J.D. and Opdyke, P.D., 1967. Antarctic Radiolaria, magnetic reversals, and climatic change: *Science*, no. 158, p. 1001.
- Heezen, B.C. and Tharp, M., 1972. Morphology of the sea floor. In Folio 16, Antarctic Map Folio Series: New York (Am. Geogr. Soc.).
- Herron, E.M., 1971. Crustal plates and sea floor spreading in the southeastern Pacific. In *Antarctic Oceanology I*, Antarctic Res. Ser.: Am. Geophys. Union, p. 229-237.
- Hollister, C.D. and Heezen, B.C., 1972. Geologic effects of ocean bottom currents. In Gordon, A.L. (Ed.), *Studies in physical oceanography*, v. 12: New York (Fordon & Breach), p. 37-66.
- Horn, D.R., Horn, B.M., and Delach, M.N., 1968. Correlation between acoustical and other physical properties of deep sea cores: *J. Geophys. Res.*, v. 73, p. 1939-1957.
- Kennett, J.P., Burns, R.E., Andrews, J.E., Chaukin, M., Jr., Davies, T.A., Dumitrica, P., Edwards, A.R., Galehouse, J.S., Packham, G.H., and van der Lingen, G.J., 1972. Australian-Antarctic continental drift, paleocirculation changes and Oligocene deep sea erosion: *Nature*, v. 239, p. 51-55.
- LeMasurier, W.E., 1972. Volcanic record of Cenozoic glacial history of Marie Byrd Land. In Adie, R.J. (Ed.), *Antarctic geology and geophysics*: Oslo (Universitetsforlaget), p. 251-259.
- Margolis, S.V. and Kennett, J.P., 1970. Antarctic deep sea cores: *Science*, v. 170, p. 1085-1087.
- McCollum, D.W., 1975. Leg 28 diatoms. In Hayes, D.E., Frakes, L.A., et al., *Initial Reports of the Deep Sea Drilling Project*, Volume 28: Washington (U.S. Government Printing Office), p. 515-571.
- Paster, T.P., 1971. Petrologic variations within submarine basalt pillows of the South Pacific Ocean. In Reid, J.L. (Ed.), *Antarctic Oceanology I*, v. 15, Antarctic Research Series: Am. Geophys. Union.
- Pitman, W.C., Herron, E.M., and Heirtzler, J.R., 1968. Magnetic anomalies in the Pacific and sea floor spreading: *J. Geophys. Res.*, v. 73, p. 2069-2085.
- Reid, J.L. and Nowlin, W., 1971. Transport of water through the Drake Passage: *Deep-Sea Res.*, v. 18, p. 51-64.
- Rutford, R.H., Craddock, C., White, C.M., and Armstrong, R.L., 1972. Tertiary glaciation in the Jones Mountains. In Adie, R.J. (Ed.), *Antarctic geology and geophysics*: Oslo (Universitetsforlaget), p. 239-243.
- Sclater, J.G., Anderson, R.N., and Bell, M.L., 1971. Elevation of ridges and evolution of the Central Eastern Basin: *J. Geophys. Res.*, v. 76, p. 7888.
- Stewart, R.J., Natland, J.H., and Glassley, W.R., 1973. Petrology of volcanic rocks recovered on DSDP Leg 19 from the North Pacific Ocean and the Bering Sea. In Creager, J.S., Scholl, D.W., et al., *Initial Reports of the Deep Sea Drilling Project*, Volume 19: Washington (U.S. Government Printing Office), p. 615-628.
- Sclater, J.G., Anderson, R.N., and Bell, M.L., 1971. Elevation of ridges and evolution of the central eastern Pacific: *J. Geophys. Res.*, v. 76, p. 7888-7915.
- Weissel, J.K. and Hayes, D.E., 1972. Magnetic anomalies in the southeast Indian Ocean, In *Antarctic Oceanology II*, Antarctic Res. Ser.: Am. Geophys. Union, p. 165-196.
- Yeats, R.S., Forbes, W.C., Heath, G.R., and Scheidegger, D.F., 1973. Petrology and geochemistry of DSDP Leg 16 basalts eastern equatorial Pacific. In van Andel, T.H., Heath, G.R., et al., *Initial Reports of the Deep Sea Drilling Project*, Volume 16: Washington (U.S. Government Printing Office), p. 617-640.

Explanatory notes in Chapter 2.





Hole 322, Core 4

Cored Interval: 352.0-361.5 m

AGE	ZONE	FOSSIL CHARACTER			SECTION	METERS	LITHOLOGY	DEFORMATION	LITHO.SAMPLE	LITHOLOGIC DESCRIPTION
		FOSSIL	ABUND.	PRES.						
LATE MIOCENE/EARLY PIOCENE	(D) <i>Denticula hustedtii</i>				0		VOID			<u>CLAYSTONE WITH SILTSTONE AND SANDSTONE</u> CLAYSTONE, SILTSTONE, SANDSTONE: dark greenish gray (5GY 4/1) and grayish green (5G 5/2). Some uneven layering. Composition <u>Claystone</u> : 84% clay mins., 7% diatoms, 6% qtz. Composition <u>Siltstone</u> : 73% qtz., 10% clay mins., 8% fldspr., 6% heavy mins. CLAYSTONE: dark greenish gray (5G 4/1). Composition: 80% clay mins., 10% diatoms, 7% qtz. (0% CaCO ₃ at 23 cm, Sect. 2 - shipboard determination). CLAYSTONE WITH INTERBEDDED SILTSTONE AND SANDY SILTSTONE: dark greenish gray (5G 4/1), slightly mottled. Composition <u>Sandstone</u> : 55% qtz., 25% fldspr., 10% heavy mins., 5% clay mins., 5% rock frags.
		R	R	M					**	
		R	R	P	1	0.5			x	
		D	F	G				*		
		D	R	M		1.0		*		
								*		
								GC		
		D	F	M	2			*		
		D	R	M				x		
								GC		
	(D) <i>Denticula lauta</i> (>5.5 m.y.B.P.)	R	R	P						
		D	F	M	Core Catcher					

BULK X-RAY		
	Siltstone 1: 65-69	Claystone 2: 110-112
Amorph.	54.0%	57.0%
Crystal.	46.0%	43.0%
Percent of Crystalline Component		
Quartz	30.1%	19.1%
K-Fldspr.	2.8%	2.7%
Plag.	33.0%	32.0%
Kaol.	0.7%	1.0%
Mica	5.9%	10.2%
Chlorite	5.7%	6.7%
Mont.	18.3%	26.1%
Clinop.	0.7%	3.6%
Amphi.	1.6%	1.7%

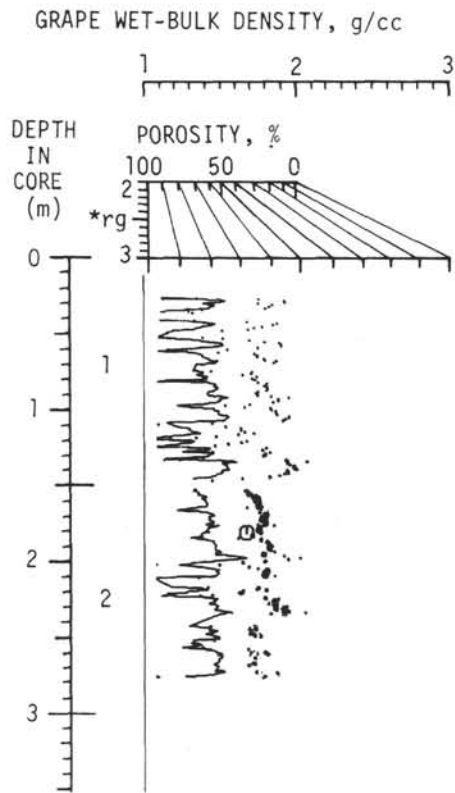
Hole 322, Core 5

Cored Interval: 390.0-399.5 m

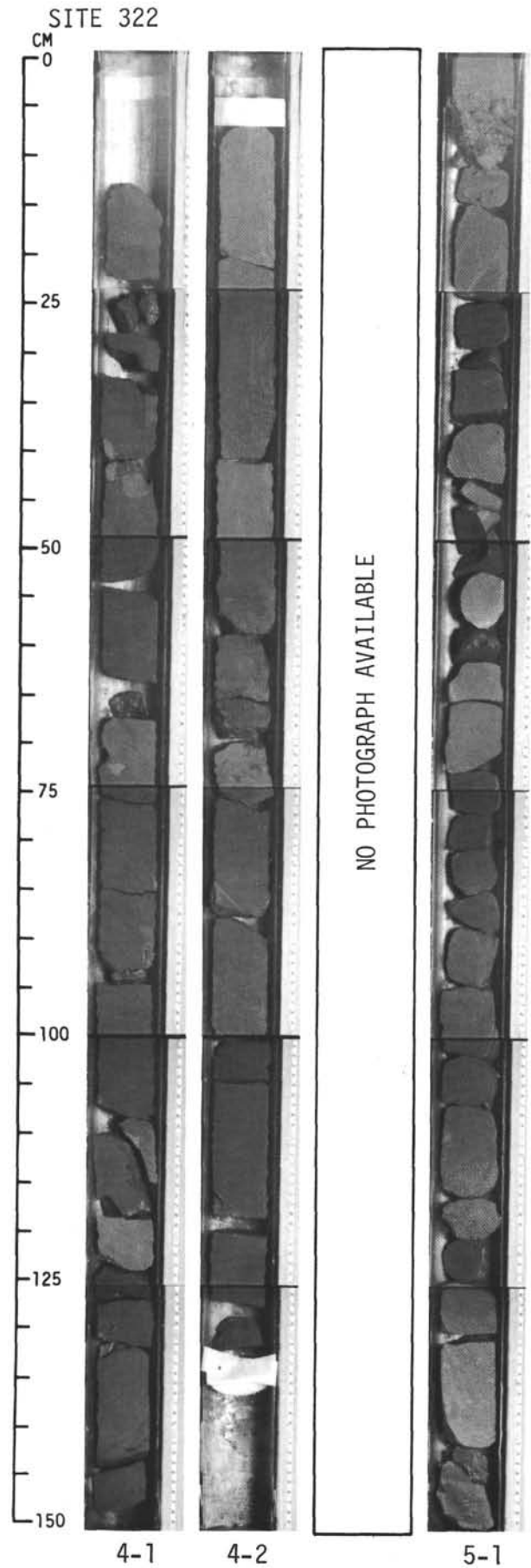
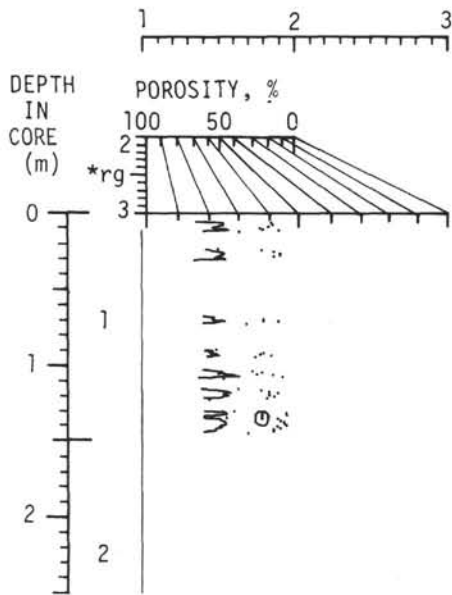
AGE	ZONE	FOSSIL CHARACTER			SECTION	METERS	LITHOLOGY	DEFORMATION	LITHO.SAMPLE	LITHOLOGIC DESCRIPTION
		FOSSIL	ABUND.	PRES.						
?	(Barren)	D	-	-	0		VOID	X		<u>SILTY CLAYSTONE</u> SILTY CLAYSTONE: dark greenish gray with abundant grayish green (10G 4/2, 10GY 5/2) clay galls (<4 mm). Scattered black spots may be micronodules of MnO ₂ . Composition: 55% clay mins., 35% qtz., 7% fldspr., 2% heavy mins. SILTY CLAYSTONE: grayish green (5G 5/2).
		D	-	-	1	0.5		**		
		R	-	-						
		D	-	-						
		P	-	-						
		R	-	-						
		Core Catcher								

BULK X-RAY (1: 76-77)			
Amorph. 34.6%	Crystal. 45.4%		
Percent of Crystalline Component			
Quartz	21.2%	Chlorite	4.0%
K-Feldspr.	5.9%	Mont.	20.6%
Plag.	36.1%	Clinop.	3.6%
Mica	6.9%	Amphi.	1.7%

Explanatory notes in Chapter 2



— = Pre-Path Length Adjustment
 ... = Post-Path Length Adjustment
 ⊙ = 2-Minute Count
 *rg = grain density, g/cc



Hole 322, Core 6

Cored Interval: 437.5-447.0 m

AGE	ZONE	FOSSIL CHARACTER			SECTION	METERS	LITHOLOGY	DEFORMATION	LITHO. SAMPLE	LITHOLOGIC DESCRIPTION
		FOSSIL	ABUND.	PRES.						
MIOCENE	?	(Barren)	D	—	0		VOID	X		<u>CLAYSTONE AND SAND</u> CLAYSTONE: dark yellow brown (10YR 4/2) with pods of very pale orange (10YR 8/2) consolidated clayey silt. (Top 25 cm mixed.) SAND: dark gray (N3), rich in heavy minerals, unconsolidated, probably disturbed, contains fragments of dark greenish gray (5G 4/1) claystone. Composition: 45% qtz., 25% heavy mins., 15% rock frags., 13% fldspr. CLAYSTONE: dusky yellow green (5GY 5/2) with pods of very pale orange (10YR 8/2) clayey silt, 95% clay, 5% silt. CLAYSTONE: dark greenish gray (5G 4/1). Composition: 86% clay mins., 8% qtz., 4% fldspr.
			D	—	1	0.5			*	
			R	—	1	1.0			*	
			D R D F	F R R	P P M	Core Catcher			*	

Hole 322, Core 7

Cored Interval: 447.0-456.5 m

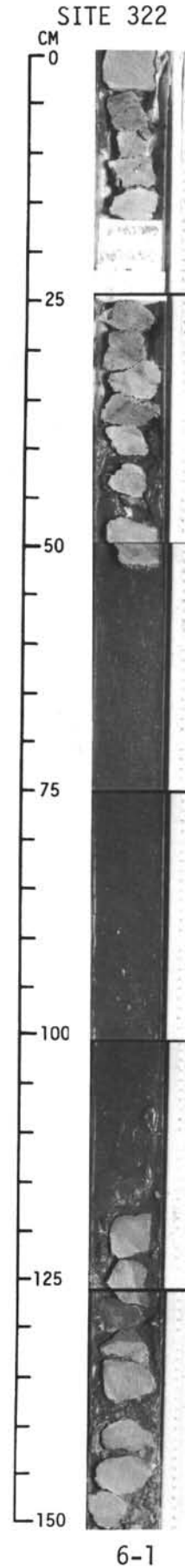
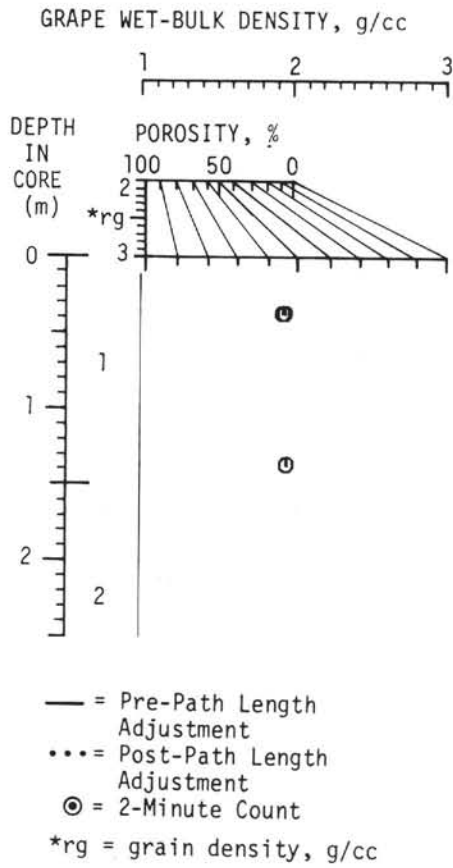
AGE	ZONE	FOSSIL CHARACTER			SECTION	METERS	LITHOLOGY	DEFORMATION	LITHO. SAMPLE	LITHOLOGIC DESCRIPTION
		FOSSIL	ABUND.	PRES.						
MIOC.			I	I	0				*	<u>QUARTZ SAND, SAND AND CLAY PEBBLES</u> Recovery consisted of only a 300-350g core-catcher sample containing dark gray (N3) well sorted COARSE SAND, greenish gray (5G 5/2) and dark greenish gray (5G 4/1) fine CLAY GRAVEL, greenish gray (5G 5/2) CLAY PEBBLES, and dark gray (N3) QUARTZ SAND PEBBLES. Sand composition: 69% qtz., 15% heavy mins., 10% rock frags., 4% opaque mins., 2% fldspr.
			I	I	Core Catcher				*	

Hole 322, Core 8

Cored Interval: 456.5-466.0 m

AGE	ZONE	FOSSIL CHARACTER			SECTION	METERS	LITHOLOGY	DEFORMATION	LITHO. SAMPLE	LITHOLOGIC DESCRIPTION
		FOSSIL	ABUND.	PRES.						
MIOC.			R	F	0				*	<u>CLAYSTONE</u> Recovery consisted of only a 40-60g core catcher sample containing yellowish brown (10YR 5/4) CLAYSTONE of 90% clay, 10% silt. Composition: 98% clay mins., 2% qtz.
			F	M	Core Catcher				*	

Explanatory notes in Chapter 2

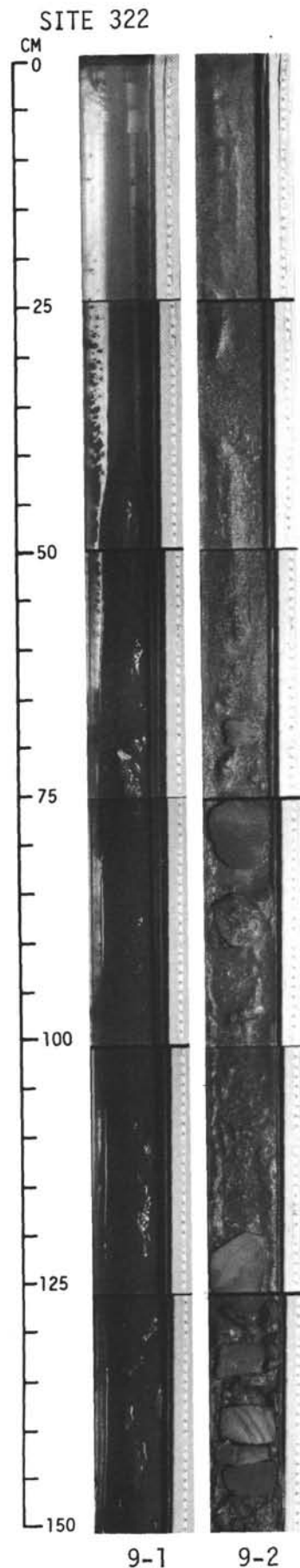
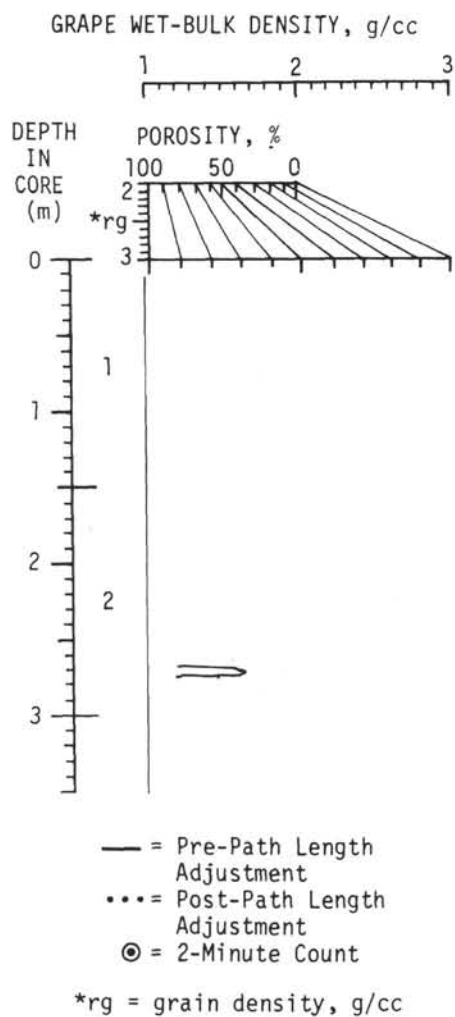


Hole 322, Core 9

Cored Interval: 466.0-475.5 m

AGE	ZONE	FOSSIL CHARACTER			SECTION	METERS	LITHOLOGY	DEFORMATION	LITHO. SAMPLE	LITHOLOGIC DESCRIPTION																								
		FOSSIL	ABUND.	PRES.																														
MIOCENE		R	F	P	0	VOID	X																											
					1	0.5						<u>SAND WITH SILTY SANDSTONE AND CLAYSTONE PIECES</u>																						
						1.0						SAND: greenish black (5G 2/1), unconsolidated, completely mixed by drilling process. Composition: 30% rock fragments, 30% fldspr., 28% qtz., 10% heavy mins.																						
					2							SILTY SANDSTONE: dark greenish gray (5G 4/1) to olive black (5Y 2/1).																						
												SAND: greenish black (5G 2/1). Composition as in Sect. 1.																						
		R P,R	R —	P —	Core Catcher					SILTY SANDSTONE: dark greenish gray (5G 4/1) to greenish black (5G 2/1). Composition as Sect. 2, 70-80 cm, (0% CaCO ₃ , 140 cm - shipboard determination). SANDSTONE: medium dark gray (N3, N4). Composition: 34% rock frags., 23% heavy mins., 23% fldspr., 18% qtz., 2% opaque mins. CLAYSTONE: grayish green (10G 4/2).																								
<p>BULK X-RAY (2: 140-142)</p> <table><tr><td>Amorph.</td><td>43.6%</td><td>Crystal.</td><td>56.4%</td></tr><tr><td colspan="4">Percent of Crystalline Component</td></tr><tr><td>Quartz</td><td>26.7%</td><td>Chlorite</td><td>1.9%</td></tr><tr><td>K-Feldspr.</td><td>8.5%</td><td>Mont.</td><td>11.1%</td></tr><tr><td>Plag.</td><td>46.1%</td><td>Clinop.</td><td>0.9%</td></tr><tr><td>Mica</td><td>3.4%</td><td>Amphi.</td><td>1.4%</td></tr></table>											Amorph.	43.6%	Crystal.	56.4%	Percent of Crystalline Component				Quartz	26.7%	Chlorite	1.9%	K-Feldspr.	8.5%	Mont.	11.1%	Plag.	46.1%	Clinop.	0.9%	Mica	3.4%	Amphi.	1.4%
Amorph.	43.6%	Crystal.	56.4%																															
Percent of Crystalline Component																																		
Quartz	26.7%	Chlorite	1.9%																															
K-Feldspr.	8.5%	Mont.	11.1%																															
Plag.	46.1%	Clinop.	0.9%																															
Mica	3.4%	Amphi.	1.4%																															

Explanatory notes in Chapter 2

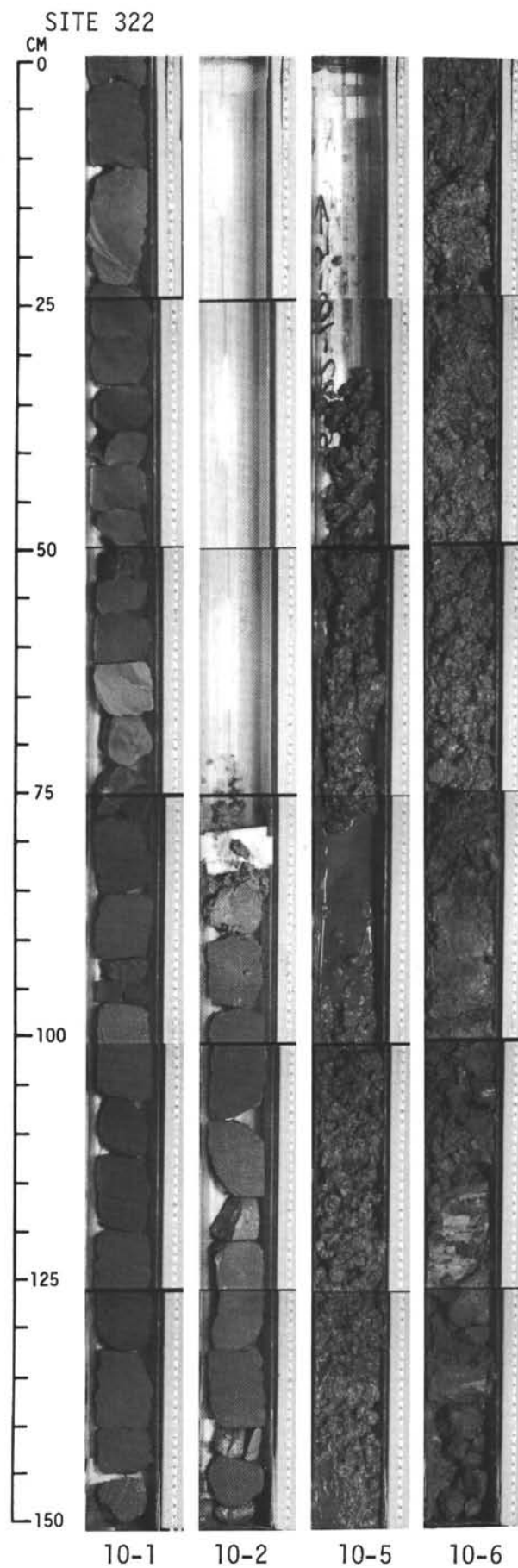
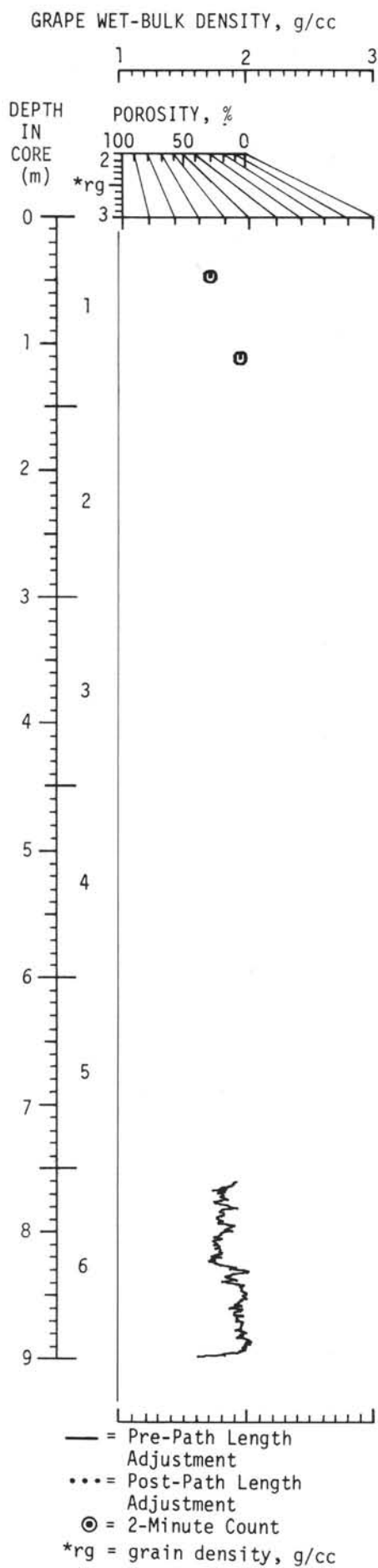


Hole 322, Core 10

Cored Interval: 485.0-494.5 m

AGE	ZONE	FOSSIL CHARACTER			SECTION	METERS	LITHOLOGY	DEFORMATION	LITHO. SAMPLE	LITHOLOGIC DESCRIPTION																																				
		FOSSIL	ABUND.	PRES.																																										
?	(Barren)	R	—	—	0				GC	<p><u>SILTY SANDSTONE AND CLAYSTONE</u></p> <p>LARGE CLAYSTONE CLASTS IN SILTY SANDSTONE MATRIX: dark gray (N3) and dark greenish gray (5G 4/1). Composition: 40% qtz., 28% rock frags., 12% fldspr., 10% heavy mins., 10% clay mins.</p> <p>SILTY CLAYSTONE: greenish black (5G 2/1). Composition: 65% clay mins., 22% qtz., 10% fldspr. Grain size: 1-50 (0-28-72).</p> <p>SILTY SANDSTONE: dark gray (N3), dark and light layers, dark layers less indurated, cross-bedding. Composition: 40% rock frags., 36% qtz., 15% fldspr., 8% heavy mins. Grain size: 1-108 (52-36-12).</p> <p>BULK X-RAY</p> <table><thead><tr><th></th><th>1: 49-50</th><th>1: 106-107</th></tr></thead><tbody><tr><td>Amorph.</td><td>54.9%</td><td>38.9%</td></tr><tr><td>Crystal.</td><td>45.1%</td><td>61.1%</td></tr><tr><td colspan="3">Percent of Crystalline Component</td></tr><tr><td>Quartz</td><td>21.7%</td><td>30.2%</td></tr><tr><td>K-Fldspr.</td><td>10.2%</td><td>10.8%</td></tr><tr><td>Plag.</td><td>27.3%</td><td>41.4%</td></tr><tr><td>Mica</td><td>12.9%</td><td>1.9%</td></tr><tr><td>Chlorite</td><td>6.8%</td><td>1.6%</td></tr><tr><td>Mont.</td><td>17.3%</td><td>12.3%</td></tr><tr><td>Clinop.</td><td>2.6%</td><td>1.0%</td></tr><tr><td>Amphi.</td><td>1.2%</td><td>0.8%</td></tr></tbody></table> <p>CLAYSTONE (DRILL CUTTINGS): dark greenish gray (5GY 4/1) mixed with pieces of more dense greenish gray (5G 6/1) clay.</p> <p>Clay is a more dense olive black (5Y 2/1) below 80 cm, Sect. 6.</p> <p>SILTY SANDSTONE: greenish black (5G 2/1). Composition: 20% qtz., 30% fldspr., 21% heavy mins., 15% rock frags., 2% opaques.</p>		1: 49-50	1: 106-107	Amorph.	54.9%	38.9%	Crystal.	45.1%	61.1%	Percent of Crystalline Component			Quartz	21.7%	30.2%	K-Fldspr.	10.2%	10.8%	Plag.	27.3%	41.4%	Mica	12.9%	1.9%	Chlorite	6.8%	1.6%	Mont.	17.3%	12.3%	Clinop.	2.6%	1.0%	Amphi.	1.2%	0.8%
						1: 49-50	1: 106-107																																							
					Amorph.	54.9%	38.9%																																							
					Crystal.	45.1%	61.1%																																							
					Percent of Crystalline Component																																									
					Quartz	21.7%	30.2%																																							
					K-Fldspr.	10.2%	10.8%																																							
					Plag.	27.3%	41.4%																																							
					Mica	12.9%	1.9%																																							
					Chlorite	6.8%	1.6%																																							
					Mont.	17.3%	12.3%																																							
					Clinop.	2.6%	1.0%																																							
Amphi.	1.2%	0.8%																																												
0.5				*																																										
1				*																																										
1.0				*																																										
2		VOID		*																																										
3		VOID																																												
4																																														
5				*																																										
6		DRILL CUTTINGS		*																																										
Core Catcher				*																																										

Explanatory notes in Chapter 2

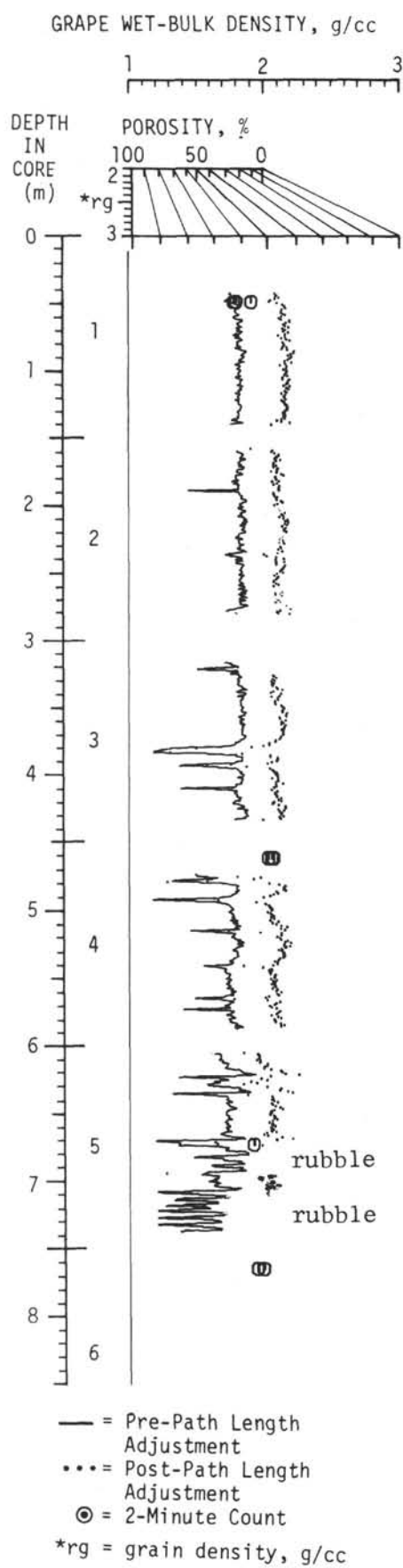


Hole 322, Core 11

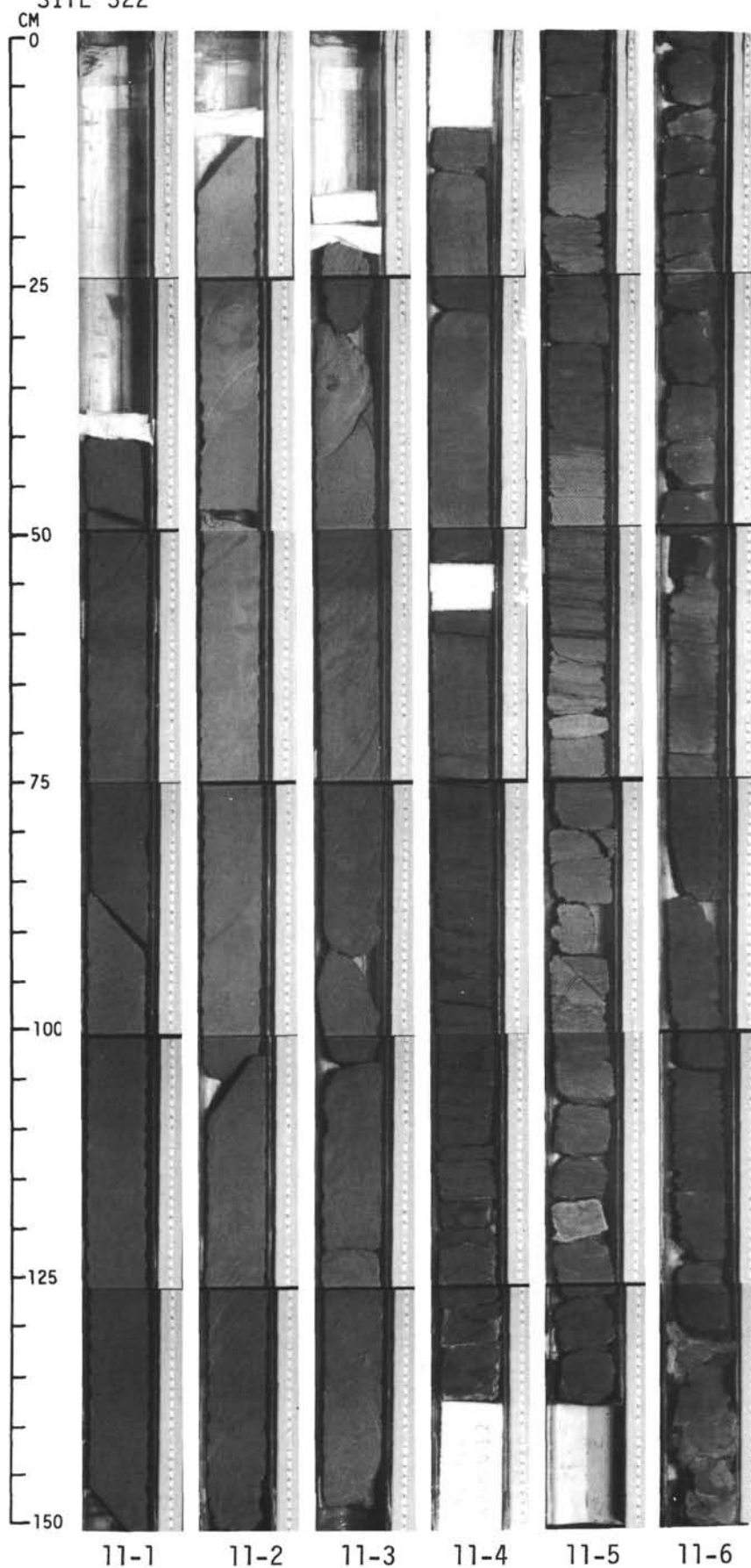
Cored Interval: 504.0-513.5 m

AGE	ZONE	FOSSIL CHARACTER			SECTION	METERS	LITHOLOGY	DEFORMATION	LITHO. SAMPLE	LITHOLOGIC DESCRIPTION
		FOSSIL	ABUND.	PRES.						
?	(Barren)				0		VOID	X		<u>SILTY SANDSTONE AND CLAYSTONE</u>
		F	—	—	1	0.5 1.0			*	SILTY SANDSTONE: dark gray (N3), very hard. Composition: 30% rock frags., 25% qtz., 20% fldspr., 12% clay mins., 10% heavy mins., 2% opaques. Grain size: 1-83 (59-26-15).
		F	—	—	2		VOID	X		Grain size: 2-43 (59-26-15).
		F	—	—	3		VOID	X		Composition (147 cm, Sect. 2): 45% rock frags., 25% qtz., 12% heavy mins., 11% fldspr., 5% authigenic(?) analcite in vertical "cracks". Grain size: 2-127 (62-23-15). Faint vertical layering, bottom of Sect. 2, top of Sect. 3.
		D	—	—	4		VOID	X		Grain size: 3-105 (64-21-15).
		F, D	—	—	4				*	Grain size: 4-24 (64-21-15). SILTY CLAYSTONE: medium dark gray (N4), 40% silt, faintly laminated. Composition: 35% clay mins., 28% qtz., 25% fldspr., 5% heavy mins., 5% rock frags. (0% CaCO ₃ at 124 cm. Sect. 4 - shipboard determination). CLAYSTONE: dark greenish gray (5GY 4/1), laminated.
		D	—	—	5				GC	CLAYSTONE: olive gray (5Y 4/1, 5Y 3/2), faintly laminated.
		F	R	P	5				*	CLAYSTONE: yellowish brown (10YR 5/4), laminated, spotted with blebs (5-10 mm) of moderate yellowish brown (10YR 4/2) clay. Some resemble burrows or fecal pellets. Grayish brown (5YR 3/2) claystone below 145 cm, Sect. 5. Composition: 97% clay mins., 1% qtz.
		F	R	P	6				GC	
		D	—	—	6				*	CLAYSTONE: same as above in rounded brecciated clasts.
?OLIGOCENE TO EARLY MIOCENE		F	R	P					*	BASALT COBBLES: very fine grained variolitic texture with clear glassy acicular laths and rectangular microphenocrysts (1-2 mm) of plagioclase. 1% iddingsite pseudomorphs after olivine (1-2 mm), <1% montmorillonite filled amygdulites (0.5 mm).
		F	R	P					*	
		F	R	P					*	
		D	—	—					*	
					Core Catcher					

Explanatory notes in Chapter 2





SITE 322



Hole 322, Core 12

Cored Interval: 513.5-523.0 m

AGE	ZONE	FOSSIL CHARACTER			SECTION	METERS	LITHOLOGY	DEFORMATION	LITHO. SAMPLE	LITHOLOGIC DESCRIPTION	
		FOSSIL	ABUND.	PRES.							
?	(Barren)	F	I	I	0		VOID	X		<u>BASALT COBBLES</u> BASALT COBBLES: drilling breccia of igneous rock with some fragments of overlying sediment and black glass. Basalt is very fine-grained variolitic and diabasic textured with clear glassy acicular laths and rectangular microphenocrysts (1-2 mm) of plagioclase. 1% iddingsite pseudomorphs after olivine (1-2 mm), <1% montmorillonite filled amygdules (0.5 mm).	
					1	0.5			+		+
						1.0					
					Core Catcher						

Hole 322, Core 13

Cored Interval: 532.5-542.0 m

AGE	ZONE	FOSSIL CHARACTER			SECTION	METERS	LITHOLOGY	DEFORMATION	LITHO. SAMPLE	LITHOLOGIC DESCRIPTION	
		FOSSIL	ABUND.	PRES.							
?	(Barren)				0		VOID			<u>BASALT COBBLES AND BRECCIA</u> BASALT COBBLES: very fine-grained variolitic and diabasic textured with clear glassy acicular laths and rectangular microphenocrysts (1-2 mm) of plagioclase. Trace amounts of montmorillonite(?) filled amygdules (0.5 mm). A few cobbles have 5-10 mm thick rinds of black glass veined with palagonite. Fractured surfaces coated with red Fe-oxides and Mn dendrites. BRECCIA: altered dark orange (10YR 6/6) and light olive (10Y 5/4) to moderate greenish yellow (10Y 7/4) volcanic fragments set in a brownish black (5YR 2/1) glassy, hyaloclastite matrix.	
					1	0.5					
						2	1.0				++
							Core Catcher				

There was no recovery in Core 14.

Explanatory notes in Chapter 2

